Lake Pavin Paleolimnology and Event Stratigraphy

Léo Chassiot, Emmanuel Chapron, Yannick Miras, Markus J. Schwab, Patrick Albéric, Aude A Beauger, Anne-Lise Develle, Fabien Arnaud, P P Lajeunesse, Renata Zocatelli, et al.

Lake Pavin Paleolimnology and Event Stratigraphy

23

Léo Chassiot, Emmanuel Chapron, Yannick Miras, Markus J. Schwab, Patrick Albéric, Aude Beauger, Anne-Lise Develle, Fabien Arnaud, Patrick Lajeunesse, Renata Zocatelli, Sylvain Bernard, Anne-Catherine Lehours, and Didier Jézéquel

Abstract

In this chapter we present an up-to-date database of sedimentary sequences retrieved from Lake Pavin during the last 50 years in both oxic and anoxic waters. The detailed history of this mid Holocene crater lake can be reconstructed from the correlation of radiocarbon dated sedimentary sequences retrieved from the deep central basin, a subaquatic plateau and littoral environments. High-resolution measurements of sediment composition (diffuse spectral reflectance, XRF core scanning) combined with the analysis of organic matter composition and preliminary pollen and diatom assemblages investigations on selected sediment cores are used to reconstruct (i) the evolution since ca. 7000 cal BP of Lake Pavin limnology together with its radiocarbon reservoir effect and (ii) the impact of a wide range of subaquatic slope failure events. Such a multidisciplinary approach of Lake Pavin basin fill revealed contrasted sedimentation patterns just after the volcanic eruption and following the development of a dense vegetation cover along the slopes of the crater. Pavin sedimentation is rapidly and largely dominated by organic rich and finely laminated diatomite formation, but several short periods of enhanced mineral inputs might reflect the influence of wetter periods, such as the Little Ice Age. Over the last millennium two large subaquatic mass wasting events are also identified and may have significantly impacted its limnology.

L. Chassiot • P. Albéric • R. Zocatelli
ISTO Institut des Sciences de la Terre d'Orléans, Observatoire des Sciences de l'Univers en région Centre, UMR 7327 (CNRS-Université d'Orléans-BRGM), Campus Géosciences, 1A rue de la Férolerie, 45071 Orléans Cedex 2, France

E. Chapron (✉)
Present Address: ISTO Institut des Sciences de la Terre d'Orléans, Observatoire des Sciences de l'Univers en région Centre, UMR 7327 (CNRS-Université d'Orléans-BRGM), Campus Géosciences, 1A rue de la Férolerie, 45071 Orléans Cedex 2, France

Present Affiliation: GEODE UMR 5602 CNRS, Université de Toulouse 2 Jean Jaurès, 5 Allée A. Machado, 31058 Toulouse Cedex 9, France
e-mail: emmanuel.chapron@univ-tlse2.fr

Y. Miras • A. Beauger
GEOLAB UMR 6042 CNRS-Université Blaise Pascal-Maison des Sciences de l'Homme, 4 rue Ledru, 63057 Clermont-Ferrand Cedex 1, France

M.J. Schwab
GFZ, Helmholtz Zentrum Potsdam, Telegrafenberg, 14473 Potsdam, Germany

A.-L. Develle • F. Arnaud
EDYTEM Environnement, Dynamiques et Territoire de la Montagne, UMR 5204 CNRS Université de Savoie, Bâtiment Pôle Montagne, 73376 Le Bourget du Lac Cedex, France

P. Lajeunesse
CEN Centre d'études nordiques, Département de Géographie, Université Laval, Québec G1VOA6, Canada

S. Bernard
LMCM Laboratoire de Minéralogie et Cosmochimie du Museum, UMR 7202 CNRS-Museum National d'Histoire Naturelle (MNHN) USM 0205, Case Postale 52, 61 Rue Buffon, 75005 Paris, France

A.-C. Lehours
LMGE Laboratoire Micro organismes: Génome et Environnement, UMR 6023 CNRS-Université Blaise Pascale, Bâtiment de Biologie A, Les Cézeaux, Avenue des Landais, BP 80026, 63171 Aubière Cedex, France

D. Jézéquel
IPGP (Institut de Physique du Globe de Paris), Sorbonne Paris Cité, Univ. Paris Diderot, UMR 7154 CNRS, 1 rue Jussieu, 75005 Paris, France

T. Sime-Ngando et al. (eds.), *Lake Pavin*, DOI 10.1007/978-3-319-39961-4_23

Four smaller scale sedimentary events related with more limited subaquatic slope failures are in addition identified, dated and correlated with regional historical earthquakes. One slope failure event may be eventually associated with a "moderate" limnic eruption in AD 1783. Since the end of the eighteenth century, enhanced subaquatic slope instabilities (and thus a higher sensitivity to regional seismicity) may have resulted from the perturbation of subaqueous sediment pore pressure after the artificial lake level drop by ca. 4 m.

Keywords
Paleolimnology • Slope failures • Sedimentary event • Natural hazard • Crater lake

23.1 Introduction

While Lake Pavin limnology has been intensively studied in the past (Parts I and II, this volume), its evolution since the lake formation ca. 7000 years ago, is still poorly known. Such a reconstruction of past environmental changes in this young crater lake can be achieved through the reconstruction of its **paleolimnology** based on a multidisciplinary approach of its sedimentary archives. This chapter aims thus (i) at presenting an up to date synthesis of available long sedimentary sequences, their chronologies and sediment proxies of environmental changes retrieved in the basin of Lake Pavin and (ii) at illustrating how the integration of different aspects of earth sciences (geomorphology, sedimentology, geophysics, geochemistry and geochronology), ecology and historical archivess can provide instructive understanding of sedimentary processes and sedimentary record of environmental changes associated with climate changes, geological hazards and human activities in a lake of volcanic origin.

Maar lakes basin fills are frequently considered as key environments for paleoclimate reconstructions (Sifeddine et al. 1996; Thouveny et al. 1994; Oldfield 1996; Ariztegui et al. 2001; Brauer et al. 1999; Caballero et al. 2006; Augustinus et al. 2012; Zolitschka et al. 2013) but little is known about the triggering factors of gravity reworking phenomena and related natural hazards (Giresse et al. 1991; Truze and Kelts 1993; Bacon et al. 2002; Bani et al. 2009; Zolitschka et al. 2013). There is particularly a need to improve our understanding of subaquatic slope stabilities, since **maar** basins are frequently characterized by steep slopes, a conical morphology and no large inflows (Chap. 22, this volume). Maar bassins thus constitute peculiar environments to investigate the impact of sub-aquatic landslide(s) and the possible generation of violent waves or crater outburst(s). In a **meromictic maar** lake such as Lake Pavin (or Lake Nyos, Cameroon) where the development of a permanent anoxic deep water body (i.e. **monimolimnion**) can favor high concentrations of biogenic and mantle-derived gases (such as CO_2 and CH_4, Camus et al. 1993; Aeschbach-Hertig et al. 1999; Albéric et al. 2013), an additional natural hazard may also be related to deep water degassing (i.e. **limnic eruption**, cf. Sigurdsson et al. 1987; Schmid et al. 2005; Caracausi et al. 2009; Mott and Woods 2010).

Radiocarbon dated long sediment cores recently collected in Lake Pavin (Fig. 23.1) provide new insights on dominating sedimentary processes in a **maar** lake and environmental history of this mid latitude volcanic region of Western Europe largely exposed to the climatic influence of the Atlantic Ocean (Stebich et al. 2005; Schettler et al. 2007).

23.2 Specific Setting of Lake Pavin

The **outlet** of the lake is deeply incised into the northern walls of the crater rim (Chapron et al. 2010) and connected to the Couze Pavin, a tributary of the Allier River in the drainage basin of the Loire River (Figs. 22.1 and 23.1). The topographic drainage basin of Lake Pavin is presently densely covered by mixed deciduous/coniferous forest (Fig. 23.1) compared to nearby environments in this mid altitude region where the vegetation cover has been deeply affected by human activities (and particularly agropastoralism) since the Roman period and the Middle Age (Stebich et al. 2005; Miras et al. 2004; Lavrieux et al. 2013).

This Lake Pavin region is characterized by an oceanic-montane climate (Stebich et al. 2005; Schettler et al. 2007) with significant annual thermal amplitude (between −5 and 20 °C, mean annual temperature of 6.5 °C) and precipitations (mean annual value between 1600 and 1700 mm). Because of the morphology of its **crater rim**, Lake Pavin is protected from regional winds, and is poorly exposed to sunlight. It is thus usually frozen during winter months while its drainage basin is frequently snow covered.

Another key feature of Lake Pavin is the occurrence of underwater springs that provide oxygenated waters at around 60 m water depth within the lake (Bonhomme et al. 2011; Jézéquel et al. 2011; Albéric et al. 2013, Fig. 22.2), matching the boundary between the **monimolimnion** and the **mixolimnion** (Fig. 22.10). Not far from the subaerial outlet (occurring at 1197 m altitude), a subaquatic outlet has also been identified between 12 and 26 m water depths on multibeam bathymetric data. As summarized in Fig. 23.1 and further detailed in Chap. 22 (this volume), the isobath −26 m also matches the boundary between a littoral sedimentary environment contrasting with the accumulation of in situ **diatomite** on the gentle slopes of a subaquatic plateau

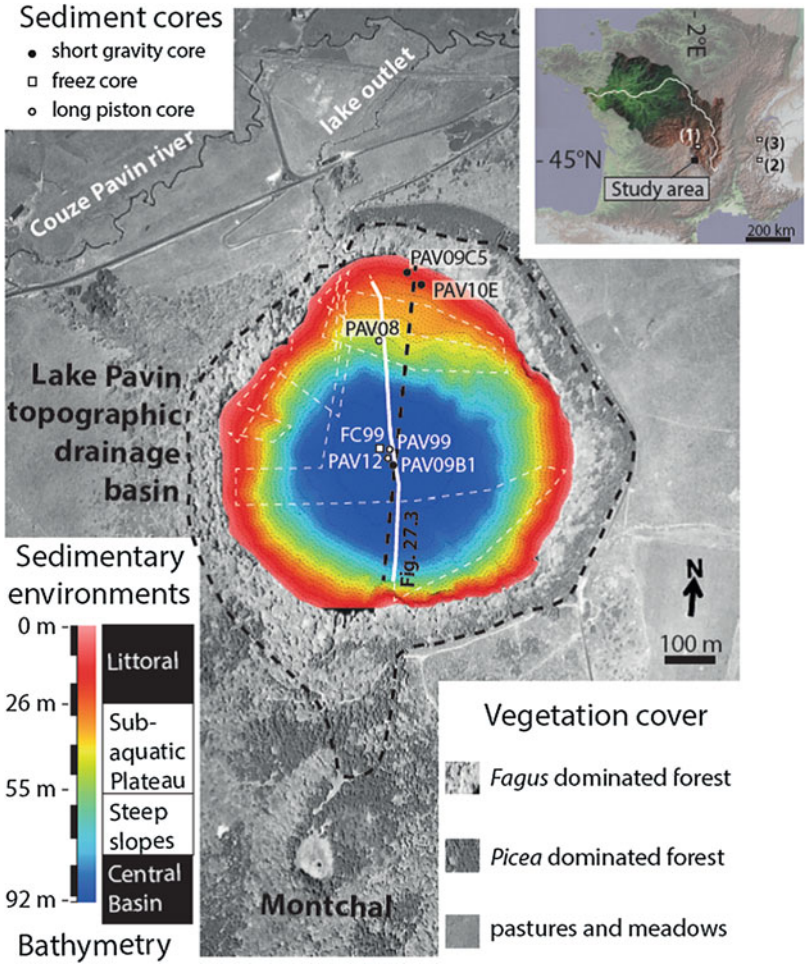

Fig. 23.1 General location of Lake Pavin in the French Massif Central (*upper right panel*) and detailed location of Lake Pavin key sediment cores discussed in the text (*central panel*). Present day vegetation cover of Lake Pavin drainage basin is also indicated. The multibeam bathymetric map and the grid of 12 kHz seismic reflection profiles (*white dotted lines*) and the 3.5 kHz seismic reflection profile (*black dotted lines*) used together with gravity, piston and freeze cores to identify four main sedimentary environments from the littoral to the deep central basin are also indicated an further presented in Chap. 22 (this volume). The location of the 12 kHz seismic profile illustrated in Fig. 23.3 is also given (*thick white line*). The general location of Lake Aydat (1), Lake Blanc Huez (2) and Lake Le Bourget (3) discussed in the text is also given

extending down to −55 m water depth in the northern part of Lake Pavin. The southern edge of this subaquatic plateau is in addition characterized by a fresh **slide scar** clearly identified on bathymetric and seismic reflection data (Figs. 22.4, 22.5 and 22.10). Finally, a 92 m deep flat central basin characterized by gas-rich sediments dominated by **diatomites** is draining steep slopes and numerous active canyons.

Such a specific hydrological and geomorphological context of Lake Pavin has to be taken into consideration when reconstructing the evolution of its limnology and surrounding environments over several millennia.

23.3 Lake Pavin Sedimentary Sequences

23.3.1 Sediment Cores and Sedimentation Rates

First short cores (<1 m long) collected in Lake Pavin were realized at the end of the '60' by divers in littoral environments and these sediment cores were sampled at site. Based on bulk sediment radiocarbon dates, Delibrias et al. (1972) discussed the age of Lake Pavin and suggested very low sedimentation rates. In the early '90', Martin et al. (1992) published, however, much higher recent accumulation rates on the plateau by 48 m water depths (between 1 and 4 mm/year) and in the deep central basin (between 0.8 and 7 mm/year) of Lake Pavin based on short gravity cores sampled at site and coupling radionuclide dating (^{210}Pb, ^{226}Ra) with cosmogenic isotope measurements (^{32}Si) on sediments.

High sedimentation rates (ranging between 1 and 3.4 mm/year over the last 700 years) were confirmed latter by Stebich et al. (2005) and Schetller et al. (2007) in the deep central basin of Lake Pavin based on sediment annual laminations (i.e. **varves**) counting with a microscope from sediment microscopic **thin-section** sub sampled on a 182 cm long gravity core (PAV 1–3) retrieved in 1999 and on a 198 cm long freeze-core (FC1) retrieved in 2001 (Fig. 23.1). Freeze-core technology (Kulbe and Niederreiter 2003) was here particularly adapted to retrieve a well-preserved sedimentary sequence in such fine-grained and gas rich lacustrine deposits accumulated in the deep and cold waters. These conditions in Lake Pavin are indeed favoring gas expansion when a sediment core is taken out of the lake.

The first long piston core PAV99 (Figs. 23.1 and 23.2) was collected in 1999 by the GFZ Potsdam in the deep central basin of Lake Pavin from an UWITEC coring platform using a 3 m long UWITEC piston corer. An 11 m long synthetic core lithology has then been established based on the correlation of overlapping split core sections retrieved at nearby locations. The study of this first long core from Lake Pavin has not yet been published, because (i) of the bad quality of sediment piston cores (due to sediment expansion by degasing) precluding the generation of good quality **thin sections** and **varve** counting, (ii) a complex succession of contrasted lithologies and (iii) a limited number of organic macro-remains found on split core sections suitable for **AMS radiocarbon** dating technics (Table 23.1).

The apparent contradiction between low sedimentation rates estimated by Delibrias et al. (1972) and higher ones identified by Martin et al. (1992) also supported by **varve** counting over several centuries (Stebich et al. 2005; Schetller et al. 2007), has only recently been explained by Albéric et al. (2013). This recent study identified an organic **radiocarbon reservoir effect** (ca. 2500 yrs) in Lake Pavin linked to its meromicticity comparing **AMS radiocarbon ages** from different organic carbon pools in the lake waters, together with **AMS radiocarbon ages** from bulk samples of organic rich lacustrine sediments and organic macro remains (leaves) from PAV08 piston core (Table 23.1). Based on this study, a **radiocarbon reservoir effect** is clearly identified over the last 1300 years at least, but is only suspected and modeled earlier because no organic macro remains were found at the base of PAV08 and could be compared to radiocarbon ages of bulk sediment samples.

PAV08 coring site is including short core PAV08-P1 presented in Chap. 22 (this volume) and is up to ca. 5 m long (Fig. 23.2). It was collected in 2008 by EDYTEM and ISTO laboratories on the subaquatic plateau by 46 m water depth (Figs. 23.1 and 23.3) from an UWITEC coring platform using either a 3 m or a 2 m long UWITEC piston corer as detailed in Chapron et al. (2010). This coring site (45°29.86'N/2°53.24'E) was selected within the **mixolimnion** of Lake Pavin based on multibeam bathymetric and seismic reflection data (Fig. 23.3 and Chap. 22, this volume).

Short gravity cores PAV10-E, PAV09-C5, and PAV09-B1 were in addition retrieved by 17.5 m, 20 m and 92 m water depth, respectively (Chap. 22, this volume). As shown in Fig. 23.2 and Table 23.1 two leave debris were dated by **AMS radiocarbon** from core PAV09-C5 (Chapron et al. 2012), and also both leave debris and bulk sediment samples from three different horizons in core PAV09-B1 (Albéric et al. 2013). These radiocarbon ages allowed dating two major **sedimentary events** in core PAV09-C5 retrieved in a littoral environment (see Chap. 22) and to document **radiocarbon reservoir effect** within the **monimolimnion** in core PAV09-B1.

During summer 2012, a 14 m long piston core (PAV12, Figs. 23.1 and 23.2) was finally retrieved by EDYTEM and LMGE laboratories from the center of the lake at the same location than core PAV09-B1 (45°29.74'N/2°53.28'E). Up to eleven samples of leaves debris and two samples of bulk sediment were recently dated by **AMS radiocarbon** (Table 23.1) in order to establish an age-depth model and to conduct a multi proxy study of contrasted sedimentary facies and successive **sedimentary events** as detailed below.

23.3.2 Sedimentary Records Within the Mixolimnion

As shown in Fig. 23.1 and further described in Chap. 22 (this issue), two main sedimentary environments are identified below the lake floor on **seismic reflection profiles** and sediment cores in Lake Pavin within its **mixolimnion**:

(i) a littoral environment (extending from the shore lines to the 26 m isobath) characterized by a transparent **acoustic facies** and a massive brownish **sedimentary facies** with some sandy layers and frequent leave debris as illustrated in cores PAV09-C5 and in the upper part of PAV10-E in Fig. 23.2 and,

(ii) *in situ* **diatomite** deposits between ca. 26 m and 55 m water depth on the subaquatic plateau developed in the northern part of the lake (Fig. 23.1). These lacustrine sediments are characterized by a faintly stratified **acoustic facies** with few low amplitude continuous **reflections** (Fig. 23.3) and a finely laminated **sedimentary facies** developing brownish and greenish laminas rich in diatoms as illustrated in PAV08 piston core (Chapron et al. 2010) and in the lower part of PAV10-E short core (Fig. 22.8).

The signature of these littoral sediments (Fig. 22.8) and diatomite sediments (Fig. 23.4), measured by **spectral diffuse reflectance** (SDR), **magnetic susceptibility** (MS) and Rock-Eval (RE) **pyrolysis** allows further characterizing the different **sedimentary units** documented by Chapron et al. (2010) in core PAV08. While SDR and MS measurements are considered as good indicators of sediment composition (Debret et al. 2010), RE **pyrolisis** is documenting organic matter geochemistry by the quantification of total organic carbon (TOC), **hydrogen index** (HI) and **oxygen index** (OI) as detailed in Behar et al. (2001) and used to precise the origin (terrestrial or lacustrine) of sedimentary organic matter in lacustrine environments as illustrated by Simonneau et al. (2013a, 2014) and Schettler and Albéric (2008).

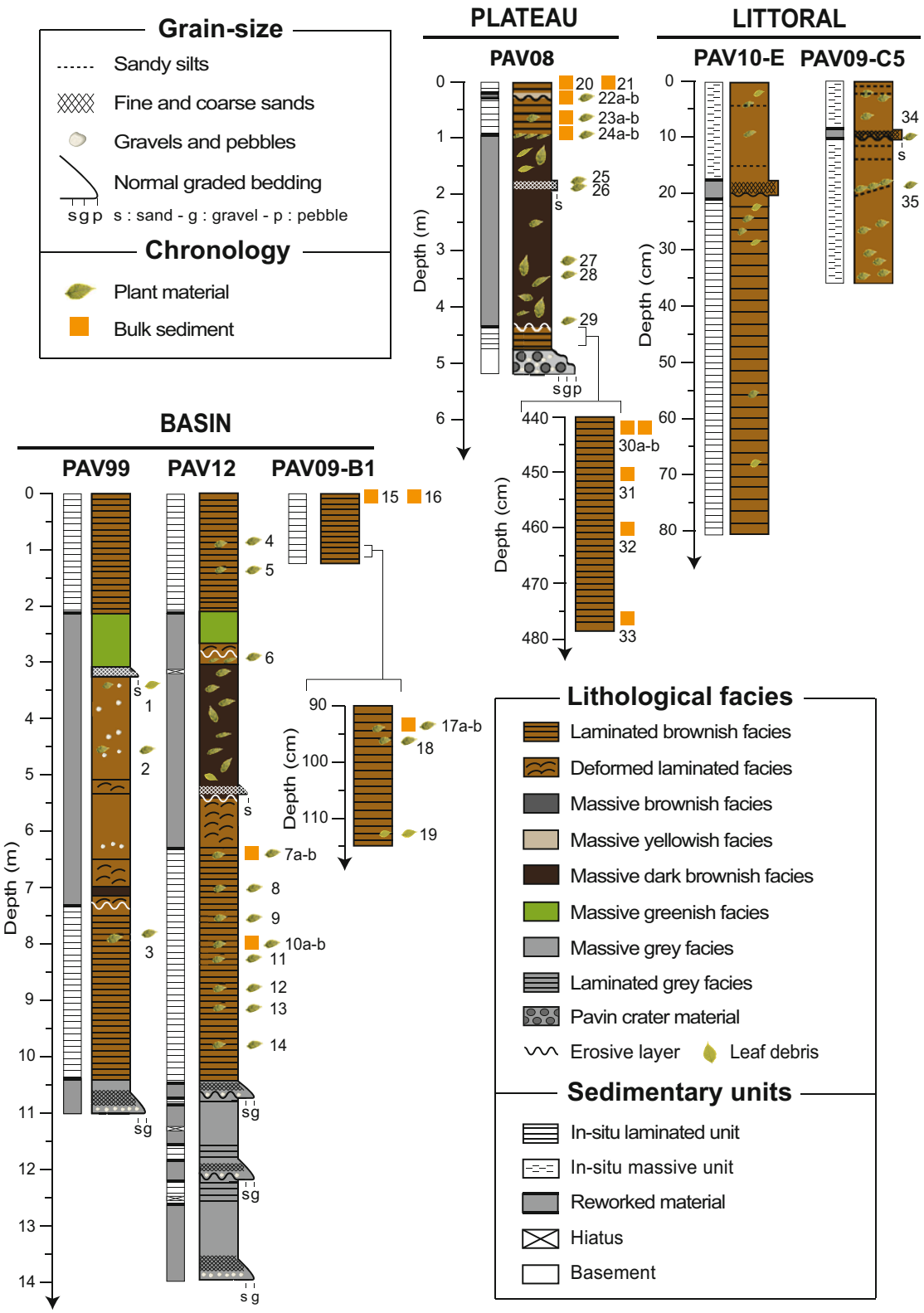

Fig. 23.2 Synthetic illustration of lithological logs of key sediment cores from Lake Pavin retrieved in the deep central basin (PAV99, PAV12, PAV09-B1), the plateau (PAV08) and littoral environments (PAV10-E and PAV09C5). The location and code of radiocarbon samples (bulk sediment or plant material) detailed in Table 23.1 are also indicated

Table 23.1 Radiocarbon dates obtained from terrestrial organic remains (leaves) or bulk organic sediment samples retrieved in sediment cores from the deep central basin, the plateau and littoral environments of Lake Pavin

Core	Depth (cm)	Laboratory reference	Material	Radiocarbon age (BP)	Reference number
PAV99	335	Poz-656	Leaves	1490 +/– 30	1
PAV99	465	Poz-657	Leaves	1700 +/– 35	2
PAV99	795	Poz-655	Leaves	2180 +/– 30	3
PAV12	81	Beta-336274	Leaves	1190 +/– 30	4
PAV12	137	Lyon-10961	Leaves	220 +/– 30	5
PAV12	287–289	Beta-336272	Leaves	2210 +/– 30	6
PAV12	645–646	SacA34984	Leaves	1730 +/– 30	7a
PAV12	645–646	SacA34985	Bulk sediment	5513 +/– 30	7b
PAV12	701	Lyon-10963	Leaves	2195 +/– 35	8
PAV12	755	Beta-336273	Leaves	2400 +/– 30	9
PAV12	798	SacA34983	Leaves	4170 +/– 30	10a
PAV12	798	SacA34997	Bulk sediment	5535 +/– 30	10b
PAV12	827	Beta-335372	Leaves	3400 +/– 30	11
PAV12	880–881	Beta-335371	Leaves	3940 +/– 30	12
PAV12	919	Beta-335370	Leaves	4400 +/–40	13
PAV12	978.5	Lyon-10962	Leaves	5250 +/– 35	14
PAV09-B1	0.5–1	SacA-28952	Bulk sediment	2965 +/– 30	15
PAV09-B1	1–1.5	SacA-28953	Bulk sediment	2445 +/– 30	16
PAV09-B1	94.5	SacA-19661	Leaves	440 +/– 35	17a
PAV09-B1	94.5	SacA-19657	Bulk sediment	6170 +/– 50	17b
PAV09-B1	96.5	Poz-33126	Leaves	150 +/– 30	18
PAV09-B1	113	Poz-33125	Leaves	1010 +/– 30	19
PAV08	0.2–0.7	SacA-19655	Bulk sediment	2070 +/– 40	20
PAV08	3–4	SacA-19656	Bulk sediment	5205 +/– 45	21
PAV08	23	Poz-31851	Leaves	1210 +/– 65	22a
PAV08	22.5–23.5	Poz-31852	Bulk sediment	3765 +/– 35	22b
PAV08	71	Poz-27046	Leaves	1290 +/– 35	23a
PAV08	70.5–71.5	SacA-19658	Bulk sediment	5960 +/– 50	23b
PAV08	97	Poz-27047	Leaves	1430 +/– 21	24a
PAV08	96.5–97.5	SacA-19659	Bulk sediment	6795 +/– 45	24b
PAV08	178.5	Poz-31849	Leaves	3180 +/– 35	25
PAV08	181	Poz-31850	Leaves	1975 +/– 35	26
PAV08	320	Poz-31848	Leaves	4350 +/– 35	27
PAV08	344	Poz-27050	Leaves	4995 +/– 35	28
PAV08	421	Poz-27051	Leaves	4820 +/– 40	29
PAV08	441–442	Poz-45411	Bulk sediment	7620 +/– 50	30a
PAV08	441–442	Poz-48070	Bulk sediment	8370 +/– 50	30b
PAV08	450–451	Poz-45413	Bulk sediment	5865 +/– 35	31
PAV08	460–461	Poz-45414	Bulk sediment	6580 +/– 40	32
PAV08	476–479	Poz-27052	Bulk sediment	6090 +/– 40	33
PAV09-C5	9	ULA-2376	Leaves	855 +/– 15	34
PAV09-C5	18	Poz-33125	Leaves	1355 +/– 35	35

Reference numbers of each date are also given in Fig. 23.2

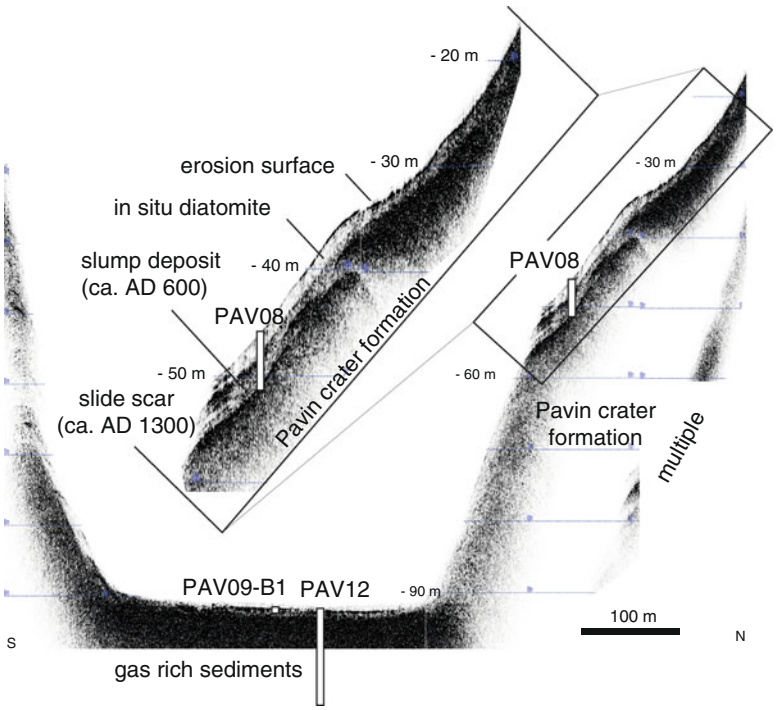

Fig. 23.3 Lake Pavin high-resolution seismic reflection profiles illustrating the development of contrasted acoustic facies above the subaquatic plateau formed by the Pavin crater formation. In the central basin, gas content in the sediment is preventing any penetration of the acoustic signal. In this part of the lake, the basin fill is thus only documented by sediment cores (PAV09-B1 and PAV12). The location of shallower core PAV08 is also indicated and allow a detail calibration of several acoustic facies associated with in situ deposits (diatomites) and reworked sediments (ca.AD 600 slump deposit and ca. AD1300 slide scar). The location of each seismic section is given in Fig. 23.1

Based on these new measurements, littoral sediments and **diatomites** are highlighting similar SDR spectrums, but littoral sediments are generally characterized by higher MS values than the **diatomites**. SDR spectrums from Lake Pavin sediments are in particular highlighting typical first derivative wavelength values of iron oxides such as Goethite characterized by higher values at 445 and 525 nm (Debret et al. 2011; Simonneau et al. 2014). TOC values between 5 and 8 % in littoral sediments are in addition generally slightly lower than the ones from the **diatomites** oscillating between 8 and 10 %.

In a former study, Chapron et al. (2010) identified two distinct **diatomite** units in core PAV08 based on their **sedimentary facies**. This distinction is further confirmed here by sediment measurements on core PAV08 clearly showing the occurrence of (Fig. 23.4):

- an upper **diatomite** unit (from the lake floor interface to 97 cm core depth) characterized by increasing TOC but decreasing HI values, and higher values of L* and b* (i.e. CIELab values of sediment reflectance, with L* parameter measuring sediment brightness, and b* parameter measuring sediment color variations from blue to yellow, cf. Debret et al. 2011);
- a lower **diatomite** unit (from 439 cm to 476 cm core depth) characterized by lower TOC values (around 8 %), higher HI (around 400 mg HC/g TOC) and darker sediments (lower L* and b* values).

Based on these high resolution measurements of sediment color and organic matter composition in PAV08, it is in addition possible to distinguish the intercalation of several contrasted layers within these **diatomites** accumulated on the plateau (Table 23.2). **Sedimentary event** 1 (E1 in Fig. 22.8) is a 2 cm thick light colored (higher L* values) layer identified at 5 cm core depth associated with an abrupt drop in TOC and HI values. **Sedimentary event** 4 (E4 in Figs. 22.8 and 23.4) is a thicker (up to 6.5 cm thick) and very similar layer (with lower TOC and HI values) easily visible on digital pictures between 17 cm and 23.5 cm core depth (Fig. 22.8). **Sedimentary event** 6 (E6 in Fig. 23.4) is a 340 cm thick dark brown layer (lower L* and b* values) rich in leave debris identified between 97 cm and 439 cm core depth. Unlike E1 and E4, E6 was previously documented in PAV08 and on seismic profiles (Chapron et al. 2010; 2012). This thick sedimentary event is developing a transparent to chaotic **acoustic facies** (Fig. 23.3) and is identified above most of the plateau (Fig. 22.5). The remarkable variability of L*, b*, TOC and HI values within E6, together with fluctuating sediment density, available **AMS radiocarbon** dates (Table 23.1) and its acoustic facies are indicating that this layer is a **slump deposit** following the classification of Mulder and Cochonat (1996). This subaquatic **slump deposit** is remolding a mixture of lacustrine and terrestrial material and is capped by a remarkable accumulation of numerous leaves and leave debris that were dated to 1290 +/– 35 ^{14}C Before Present (BP) by **AMS radiocarbon** (Table 23.1).

Two **sedimentary events** (E 5 and E6) are also identified within a littoral environment in core PAV09-C5 (Fig. 22.8): E

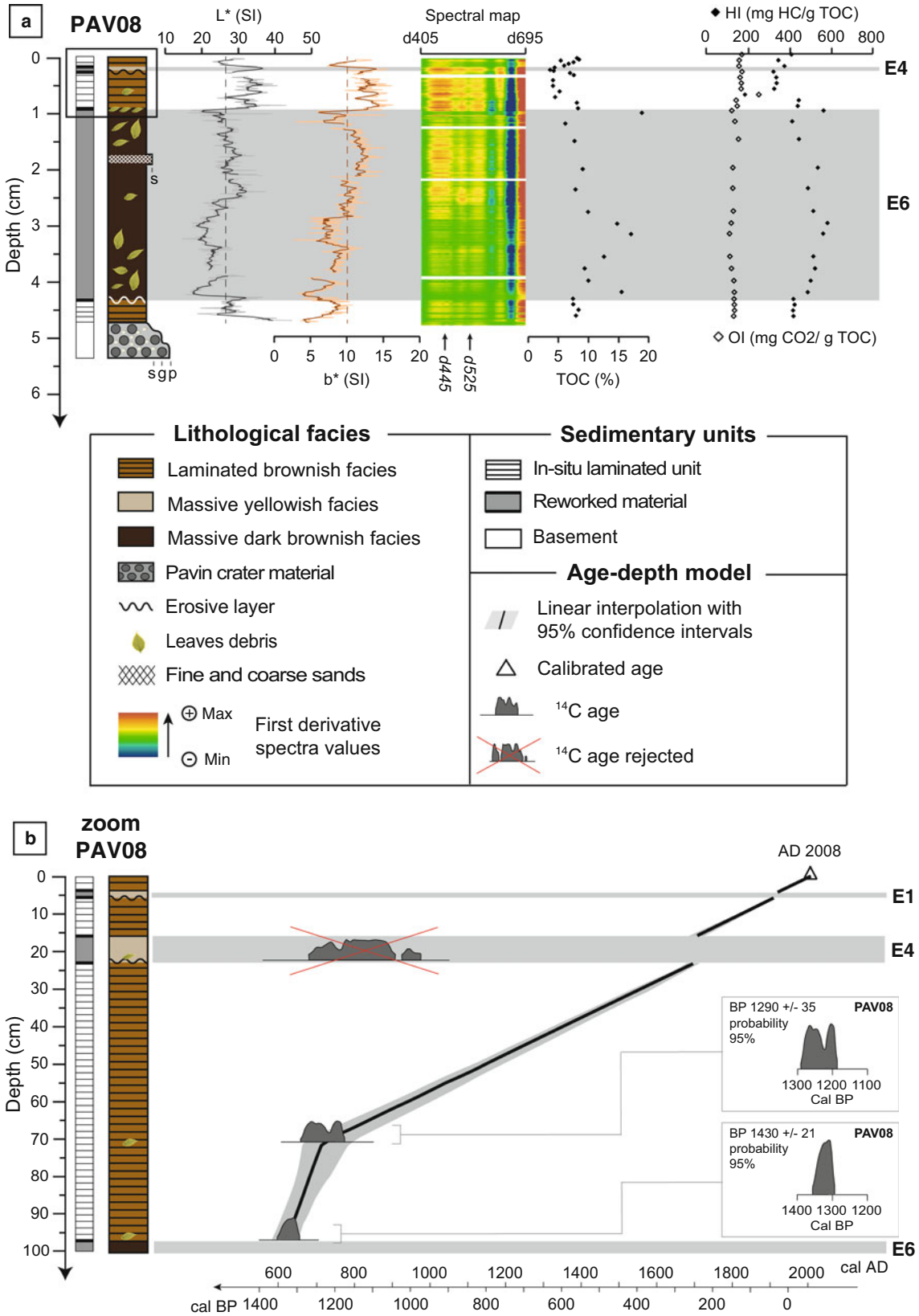

Fig. 23.4 Multi-proxies analyses on core PAV08 (**a**) and associated age-depth model of the upper unit (**b**) with calibration results with IntCal13 (Reimer et al. 2013). For continuous measurements, *thick* and *dashed lines* represent respectively a moving average and the mean. Sedimentary events E1, E4 and E6 discussed in the text are highlighted by *grey bars*

Table 23.2 Ages and thicknesses of sedimentary events identified in Lake Pavin sediment cores and possible associated historical earthquakes in the study area reported by Sisfrance data base from the French Geological Survey (BRGM)

Lake Pavin				Regional Seismicity				
Event	Core	Thickness	Age Cal AD	Historical earthquake	MSK scale intensity	Distance from Pavin	Type of event recorded in lakes	Likelihood a seismic triggering
E1	PAV08-P1	2 cm	1915 +/– 5	La Bourboule 1921	4.5	15 km		High
E2	PAV09-B1	2 cm	1880 +/– 70	Mont-Dore 1863	5	11 km	Slump in Lake Guéry (1)	Very high
				Issoire 1892	7	30 km		
E3	PAV09-B1	2 cm	1840 +/– 80	Chambon-sur-lac 1844	5.5	9 km		High
				Blesle 1833	7	30 km		
				Issoire 1833	6	30 km		
E4	PAV09-B1	1 cm	1775 +/– 90	Lepaud 1783	??	??	Limnic eruption in Lake Pavin ?	High
	PAV08	6.5 cm	1700 +/– 15	Mainsat 1783	??	??		
E5	PAV12	420 cm	1300 +/– 50	Uzerche 1348	??	??	Slumps in Lakes Guéry and Montcineyre (1,2)	High
	PAV99	510 cm	??					
	PAV09-C5	1 cm	1190 +/– 30	Limousin plateau 1233	??	??		
E6	PAV08	340 cm	620 +/– 20	No information				Moderate
	PAV09-C5	1 cm	660 +/– 50					

Also indicated is the type of contemporaneous mass wasting deposits documented in nearby lakes and further detailed (1) in Chassiot et al (in prep.) and (2) in Chapron et al (2012), as discussed in the text

5 is a 1 cm thick erosive sand layer rich in leave debris at 9 cm core depth, while E6 is a 1 cm thick layer at 18 cm core depth, very rich in leaves and also containing few pebbles and some fine sands (Chapron et al. 2012). As shown in Table 23.1, leave debris from E5 and E6 were dated by **AMS radiocarbon** to 855 +/– 15 ^{14}C BP and 1355 +/– 35 ^{14}C BP, respectively.

Using the IntCal13 radiocarbon calibration curve from Reimer et al. (2013), **AMS radiocarbon** ages ^{14}C BP can be accurately calibrated and converted in year cal BP or cal AD (Anno Domini, i.e. calendar year). This exercise is giving similar calibrated ages for E6 in core PAV08 (cal AD 717 +/– 39) and in core PAV09-C5 (cal AD 663 +/– 18). Based on their similar age clustering around AD 680, striking sediment layers identified within Lake Pavin littoral environment (at 18 cm in core PAV09-C5) and between **diatomite** deposits (from 97 cm to 439 cm in core PAV08) can be correlated and linked to a single **sedimentary event** (E6). This event E6 has different sedimentary signatures in shallower and deeper parts of the plateau, suggesting that such subaquatic sediment slumping along the plateau was probably sufficiently large and fast to generate erosive waves along the shore lines of Lake Pavin and to develop at site PAV09-C5 a coarse grained layer rich in terrestrial organic macro remains by 20 m water depth (Chapron et al. 2012).

No organic macro remains were found on top of E1 and E4 in core PAV08, but it is possible to estimate their age, based on the establishment of an age-depth model using calibrated **AMS radiocarbon** date following Reimer et al. (2013) and the depth of radiocarbon samples. Considering that these **sedimentary events** were rapidly deposited, in such age-depth model, the core depths should be, however, corrected from the thicknesses of each **sedimentary events**. Figure 23.4 B illustrates such PAV08 age-depth model based on the linear interpolation of two available dates in the upper diatomite unit using the CLAM software (Blaauw 2010). One radiocarbon age being too old was found within E4. Because this sample was likely reworked from the catchment area it can't be used to construct the age-depth model. Figure 23.4, illustrate thus the new age-depth model of the upper **diatomite** unit in PAV08 and allows dating E1 to cal AD 1915 +/–5 and E4 to cal AD 1700 +/–15 (Tables 23.1 and 23.2).

At the base of PAV08, between 476 cm and 509 cm core depth, a light grey to brownish gravels and pebbles in a coarse sand and silty matrix were sampled and analyzed (Chapron et al. 2010). Within this coarse-grained sedimentary facies, ca. 40 % in clast number consists of crystalline rocks, ca. 30 % of various trachyandesitic **lavas**, while the rest is made of basaltic looking **lavas** and of variously vesicular yellowish **pumices**. This **sedimentary facies** has been related to the Pavin crater material developing its **crater rim** and to the **acoustic substratum** on seismic reflection profiles. A sample of bulk organic rich **diatomite** sediments at 476–479 cm core depth just above the Pavin crater material has been dated by **AMS radiocarbon** and gave an age of

6090 +/−40 ^{14}C BP corresponding to 6971 +/−61 cal BP (Table 23.1). Because this age of lacustrine sediment is very close to the age of Pavin **tephra** layers found in regional outcrops and peat deposits (Chap. 6, this volume), it suggest that the onset of lacustrine sedimentation in Pavin started very quickly after the crater formation at site PAV08, without any significant **radiocarbon reservoir effect** (Albéric et al. 2013).

23.3.3 Sedimentary Records Within the Monimolimnion

All the sediment cores within the **monimolimnion** in Lake Pavin were collected in the deep central basin (Fig. 23.1) and are dominated by finely laminated **diatomites** (Fig. 23.2). Within both long piston cores PAV99 and PAV12, two distinct **diatomite** units can be identified within the two first meters below the lake floor (upper **diatomite** unit), and above ca. 1050 cm core depth were a coarse grained greyish unit characterizes the base of these piston cores (Fig. 23.2). This lower **diatomite** unit is ca. 3 m thick in PAV99 (between 730 and 1045 cm core depth), but up to ca. 4 m thick in PAV12 (between 626 and 1046 cm core depth).

The **sedimentary facies** and SDR measurements within these **diatomites** from the deep central basin are roughly similar to the ones from the plateau (Figs. 22.8, 23.4 and 23.5). RE analyses are however more variable, and generally showing lower TOC (up to 6 %) and IH (down to 200 mg HC/g TOC) values within the upper meters, while the lower unit has higher TOC (up to 18 %) and IH (oscillating around 500 mg HC/g TOC) values. Figure 23.6 is illustrating the stratigraphic correlation of available sediment cores from the central basin of Lake Pavin and the age-depth model established for PAV12 using the CLAM software (Blaauw 2010) based (i) on calibrated **AMS radiocarbon** dates on terrestrial organic macro remains found in PAV99, PAV09-B1 and PAV12 (see Table 23.1 and applying the calibration curve from Reimer et al. 2013) and (ii) on varve counting in the upper **diatomite** unit by Schettler et al. (2007) preformed on freeze core FC1. This figure shows that the upper **diatomite** unit contains several reworked organic material witch were not used for the age-depth model, while only one radiocarbon date has been removed in the lower **diatomite** unit to build up its chronology.

RE analysis (TOC and HI, Fig. 23.5) from PAV12 sediments are very different from the values obtained in core CHA13-7B retrieved in nearby Lake Chauvet central basin (Fig. 22.11). Based on the studies of Ariztegui et al. (2001), Behar et al. (2001) and Simonneau et al. (2013a), the organic matter in PAV12 samples are effectively essentially made of algae, and only few macro remains of terrestrial organic matter (leaves and leaves debris) seems therefore to characterize the organic fraction of Lake Pavin **diatomites** in the deep central basin. This is further supported by Scanning Electron Microscopy (SEM) images of selected samples from PAV12 (Fig. 23.7) illustrating the predominance of diatoms frustules and cysts more or less well-preserved within Lake Pavin sediments.

In order to further document PAV12 sediment geochemistry and provenance, X-ray fluorescence (XRF) measurements were performed on an Avaatech core scanner at EDYTEM laboratory every 5 millimeters with a Rhodium tube source. The settings were adjusted to 10 kV and 0.75 mA with an acquisition time of 20 seconds in order to measure Al to Fe relative intensities. Titanium (Ti) is for example an element relatively easy to measure and frequently used to track the evolution of clastic sediment supply in lacustrine basins (cf. Arnaud et al. 2012). Figures 23.5 and 23.8 generally illustrate low Ti content in PAV12 laminated **diatomites** and thus low clastic supply from Pavin catchment area, but several Ti peaks are however punctually identified, although maximum values in Ti are found in the light grey basal facies further detailed below.

Locally, several **sedimentary events** characterized by very high values of MS are also contrasting in core PAV09-B1 with the low MS values associated with **diatomites** in the upper unit (see E2, E3 and E4 in Fig. 22.8). These **sedimentary events** are, however, probably very punctual because they were not documented within the upper meters of other cores PAV99 (Stebich et al. 2005), FC1 (Schettler et al. 2007) and PAV12 (this study).

A major **sedimentary event** (E5) is on the contrary clearly identified in between the upper and lower **diatomite** units in both piston cores PAV99 and PAV12 (Figs. 23.2 and 23.5). In both cores this **sedimentary event** is characterized by a different thickness (up to ca. 510 cm thick in PAV99, but ca. 420 cm thick in PAV12) and a complex succession of contrasted lithological units.

In PAV99, the base of E5 consist in highly deformed **diatomites** were laminations are still visible (between ca. 730 and 650 cm core depth and between ca. 535 and 510 core depth). This deformed laminated facies is locally interrupted (i) by a massive dark brownish facies (ca. 18 cm thick) showing a sharp base around 715 cm core depth and (ii) by a massive brownish facies (between ca. 650 and 535 cm core depth) were laminations are generally destroyed or mixed and locally associated with some gravels and pebbles. Between 510 and 325 cm core depth, a similar massive brownish facies with destroyed laminations and some gravels and pebbles is again identified together with few organic macro remains (leave debris) suitable for **AMS radiocarbon** dating (Table 23.1). Above 325 cm core depth, a sharp based sandy layer ca. 4 cm thick, quickly evolves into a massive greenish facies ending at around 220 cm core depth, just below the upper diatomite unit (Fig. 23.2).

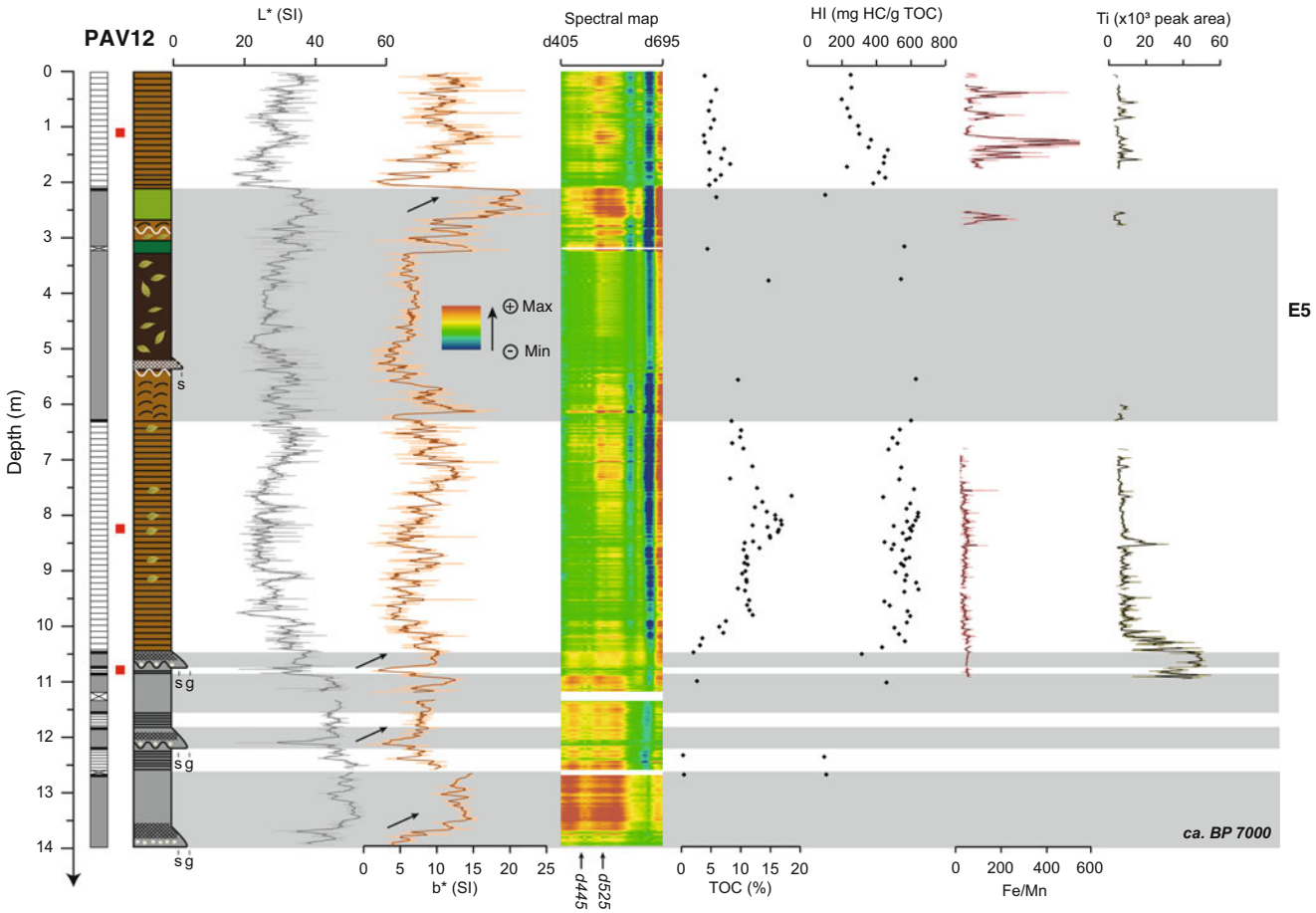

Fig. 23.5 Detailed multi-proxies analyses performed on core PAV12. *Grey squares* represent reworked material. L* and b* are parameters derived from spectrophotometric analyses. The spectral map shows first derivatives relative intensities with d445 and d525 used as proxies of iron oxides. Percent TOC and Hydrogen Index (HI) are provided by Rock-Eval 6 analyses. Ti content and Fe/Mn where measured by X-Ray Fluorescence. *Red squares* report samples for SEM images presented in Fig. 23.8. *Black arrows* are highlighting turbidites intercalated within laminated sediments (basal unit) or above a major Mass-Wasting Deposit (E5)

In PAV12, the base of E5 is characterized by a sharp transition from the lower diatomite unit towards highly deformed **diatomites** were laminations are still visible (between ca. 625 and 543 cm core depth). This facies is nicely reflected by sharply fluctuating values of b* parameter (Fig. 23.5). Between ca. 543 and 309 cm core depth, a massive dark brownish facies rich in organic macro remains (leave debris) occurs and is associated with fluctuating and lower values of L* and b* parameters. A sharp based sandy layer is in addition observed between 540 and 536 cm core depth. Between ca. 308 and 265 cm core depth another facies made of deformed **diatomites** (were some laminations are still visible) is locally interrupted by an erosive horizon rich in leaves debris. Above this contrasted facies, a massive greenish facies occurs between 265 and 207 cm core depth just below the upper **diatomite** unit (Fig. 23.5) and is characterized by a gradual increase of b* and higher content in goethite as reflected by 445 and 525 nm first derivative values.

As shown in Fig. 23.6 and detailed in Chapron et al. (2010), the top of E5 is dated to ca. 700 cal BP (ca. AD 1300) based on the extrapolation of **varve** counting from FC1 performed by Schettler et al. (2007). This chronology is now further supported by the age of two leaves debris from PAV09-B1 and PAV12 collected within the upper **diatomite** facies. Organic macro remains found within E5 either in PAV99 or PAV12 (Table 23.1) are, in addition, systematically older and not in stratigraphic order. Together with the above mentioned contrasted lithological descriptions within E5 and the occurrence of erosional surfaces within E5, these specificities imply that E5 is a major reworked deposit. According to the youngest age found at the top of the lower **diatomite** unit below E5 in PAV12 (ca. AD 300), it is also clear that this large event E5 has been erosive and probably remolded some of the previously deposited **diatomites** in the deep central basin. This is further supported by the different thickness of preserved **diatomites** below E5 within PAV99 and PAV12. Based on these arguments and following the classification of

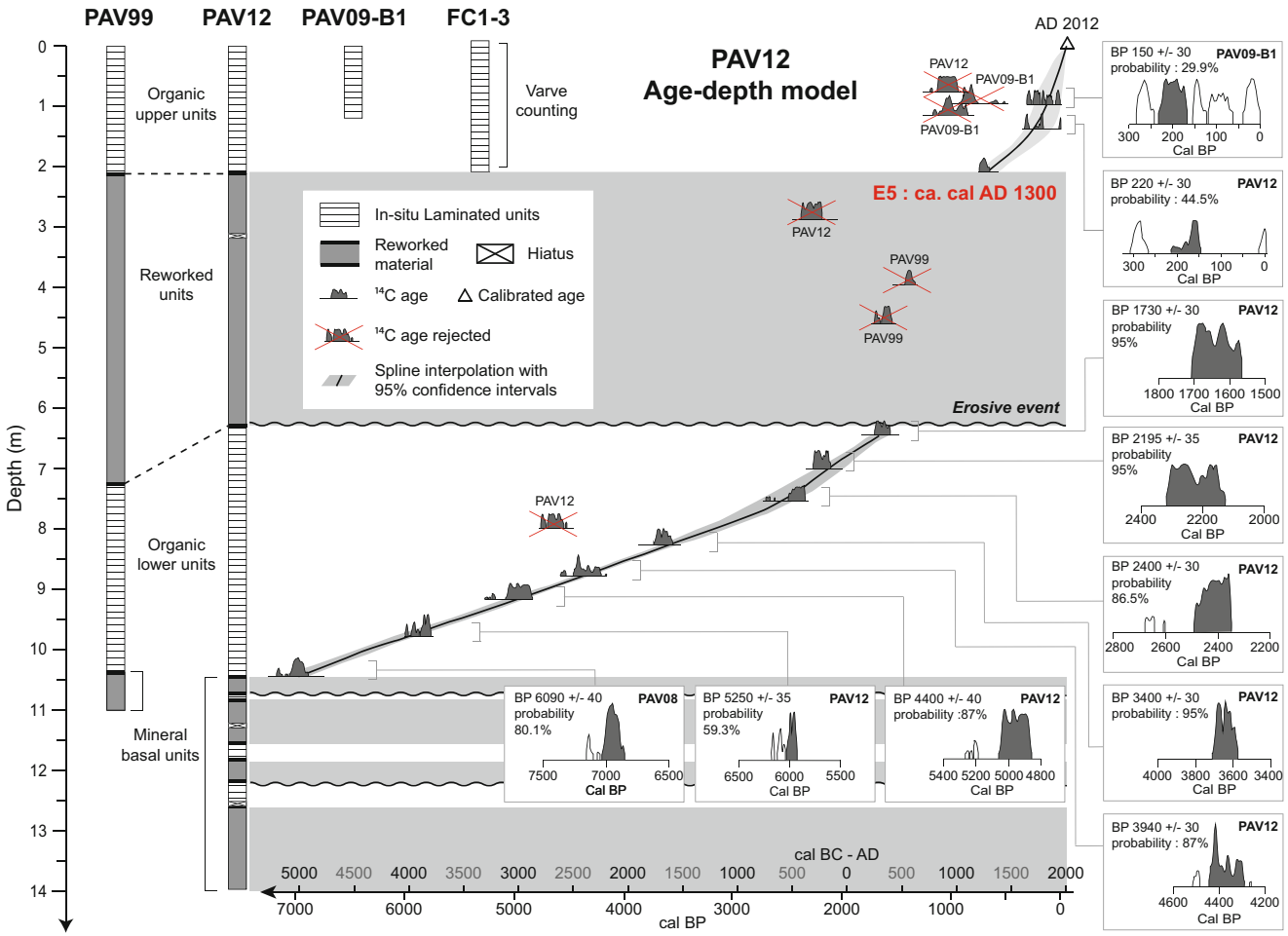

Fig. 23.6 Age depth model of core PAV12 based on AMS radiocarbon ages from organic macro remains using the Intcal09 calibration curve from Reimer et al. (2013), the identification of reworked deposits intercalated within the central basin fill and the application of a spline interpolation between the dating points using the CLAM software (Blaauw (2010). Varves counting established on a twin core retrieved from deep basin of Lake Pavin (Schettler et al. (2007) is supported by two radiocarbon dates (one from PAV09-B1 and one from PAV12). *Grey squares* correspond to reworked material associated with sedimentary events as discussed in the text

Mulder and Cochonat (1996), E5 can be subdivided in two successive mass wasting deposits: (i) first, a pluri-metric and erosive **slump deposit** remolding more or less deformed lacustrine sediments, and (ii) secondly, a pluri-decimetric greenish and fine grained **turbidite.** This **turbidite** is bearing a well-preserved and normally graded sandy base at 325 cm below the lake floor in PAV99, but is essentially made of a similar greenish and massive fine-grained sequence on both piston cores. The **slump** deposit and this fine-grained **turbidite** sequence are also clearly thinner in PAV12 than in PAV99, suggesting that the latter piston core is localized in a more proximal position than PAV12 from this mass wasting event E5. A classical fining upward pattern within the fine-grained turbiditic sequence retrieved in PAV12 is nicely illustrated by increasing b* values (Fig. 23.5). This is suggesting that this large and erosive mass wasting event remobilized and re-suspended a significant volume of lacustrine sediments within the water column, before massive settling occurred in the deep central basin of this maar lake.

Coarser but similar **turbidite** deposits are also identified in the basal grey unit retrieved in both piston cores from Lake Pavin central basin (Figs 23.2 and 23.5). These light-greyish **turbidites** are characterized by pluri-centrimetric thick sandy bases bearing some few gravel particles composed of similar volcanic materials than the Pavin crater formation retrieved at the base of PAV08. While PAV99 only contains one single **turbidite** between ca. 1050 and 1100 cm core depth, up to three similar **turbidites** are found at the base of PAV12. Their coarse-grained sandy bases are capped by a fining upward sequence that is centimetric to decimetric in thickness, fine-grained and systematically characterized by progressively increasing b* values. In PAV12, these **turbidites** are intercalated in between finely laminated and light-grey colored sediments (high L* and b* values) that are bearing low TOC and high Ti values (Fig. 23.5). It is also

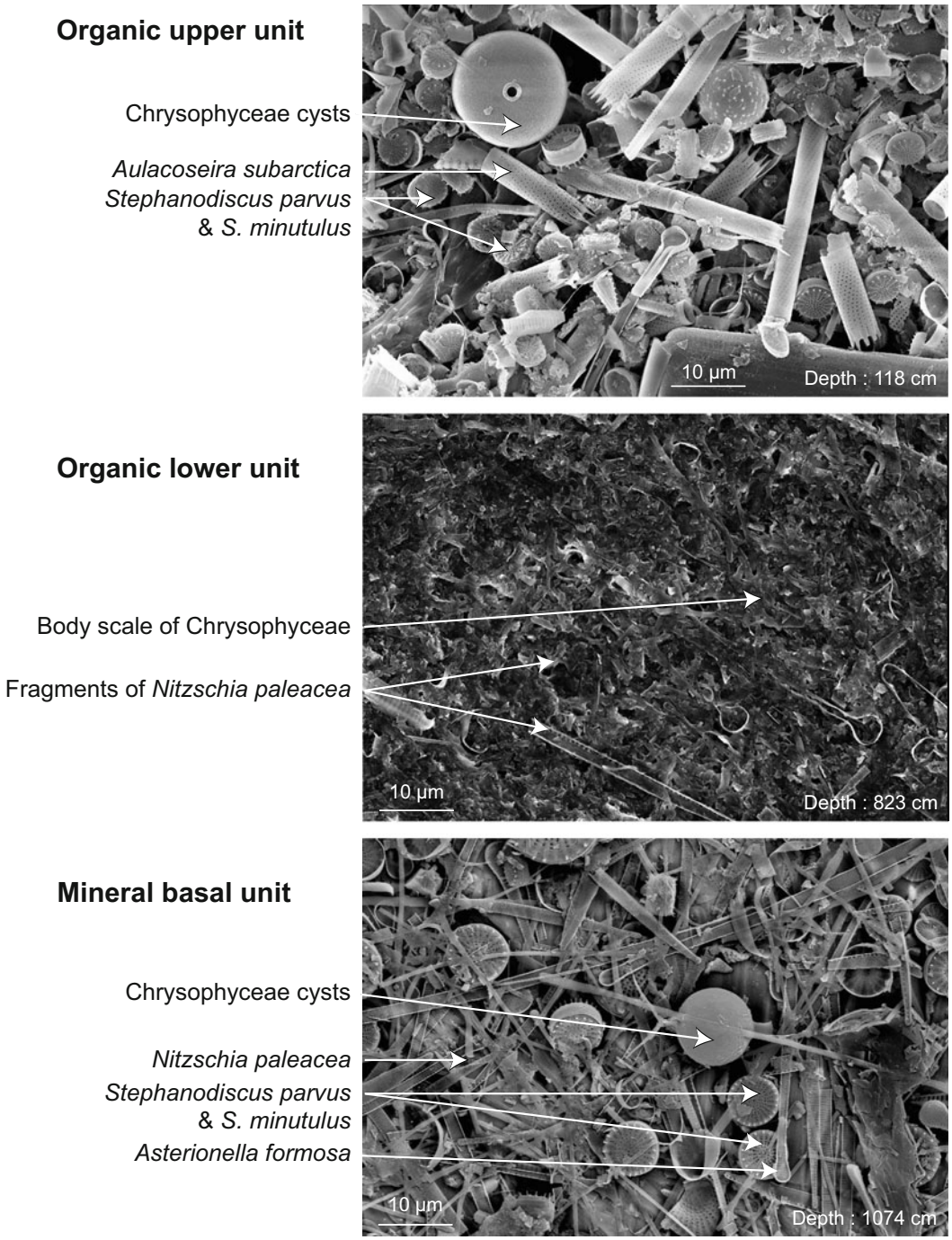

Fig. 23.7 Scanning Electron Microscopy images for PAV12 samples (*red squares* in Fig. 23.5) reflecting changes in diatoms assemblages inside the organic upper and lower units and the mineral basal unit

interesting to note that this basal mineral unit of Lake Pavin is rich in diatoms but made of different assemblages than the upper and lower **diatomite** units (Fig. 23.7) as further detailed below.

The chronology at the base of PAV12 is still poorly constrained because no organic macro remains were found in-between these light grey **turbidites** or at the base of the lower **diatomite** unit. Assuming that the onset of organic rich **diatomite** accumulation is synchronous throughout the lake and, like in PAV08, occurring around 7000 cal BP, it seems very likely that this mineral unit developed shortly after the Pavin eruption, in a recently formed maar lake. As a working hypothesis, to establish the lower boundary of the age-depth model in PAV12 with the CLAM software, one may thus use the calibrated **radiocarbon age** of bulk sediment retrieved just above the Pavin crater formation in

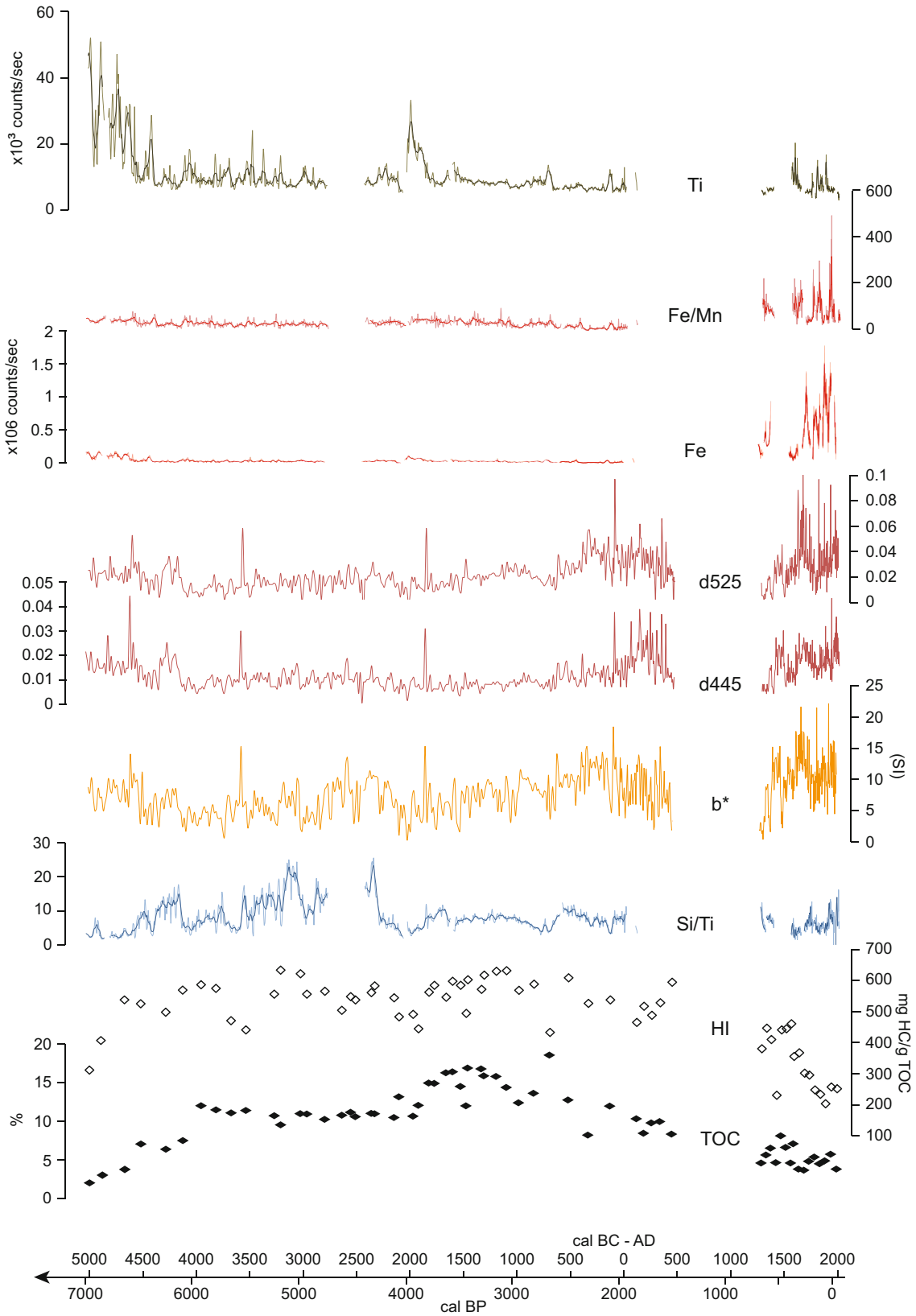

Fig. 23.8 Evolution through the last 7000 years of organic and mineral sedimentation in PAV12, as documented by geochemical proxies (Ti; Fe/Mn; Fe; Si/Ti curves form XRF core scanning), organic matter geochemistry (Hydrogen Index, HI and Total Organic Carbon, TOC) and spectrophotometric data (first derivative d445 and d525 and b* parameter)

PAV08 (Figs. 23.6, 23.2, Table 23.1). This basal turbiditic sequence seems here to have been deposited when the recently formed crater presented steep slopes surrounded by post-eruptive unsteady material, which have been quickly reworked into the deepest part of the crater.

In summary, Lake Pavin sedimentation in the central basin has been largely dominated by organic rich and finely laminated **diatomite** formation over the last ca. 7000 years. Roughly 700 years ago (ca. AD 1300), a major mass wasting event (E5) took place eroding and reworking approximately one millennia of **diatomite** deposition in the deep central basin. More recently, two smaller clastic layers (E3 and E2) only intercalated in-between the upper **diatomite** unit in a single core (PAV09-B1), can be dated to AD 1840 +/− 80 and AD 1880+/− 70, respectively, using an age-depth model with the CLAM software combining radiocarbon dating (one age from PAV09-B1 and two from PAV12) together with **varve** counting chronology established by Schettler et al. (2007) in a nearby freeze core (FC1).

23.4 Lake Pavin Stratigraphic Record of Environmental Changes

23.4.1 Lake Level Evolution in Lake Pavin

The level of Lake Pavin is controlled (i) by the altitude of its sub-aerial outlet, (ii) by the flow of its subaquatic outlet and (iii) by climate (precipitation regimes, lake water evaporation). The V-shape geomorphology of its sub-aerial outlet deeply incised into the walls of Pavin **crater rim** suggest that this maar lake has been exposed to a lake level lowering. Such morphology may result either from a progressive incision of the lake outlet into a heterogeneous and relatively poorly consolidated volcanic phreato-magmatic formation (Delbecque 1898; Chap. 5). It may also result from a relatively recent and abrupt collapse of this sector of the **carter rim** (i.e., a crater outburst) triggered either spontaneously (and induced by the weight of the lake water column) or favored (i) by a lake level rise, (ii) by the propagation of a violent wave into the lake outlet or (iii) by earthquake shaking (Chapron et al. 2010). The flow of the subaquatic outlet of Lake Pavin is poorly documented, but available data suggest it is relatively limited compared to the one of the sub-aerial outlet (Jézéquel et al. 2011). A recent synthesis by Magny et al. (2013) discussed the impact of climate on well-dated synchronous phases of lake level changes during the Holocene across Western European mountain ranges or around the Mediterranean Sea, but little is still known about the amplitudes of these lake level changes. Because such lake level reconstructions in Western Europe are typically performed in carbonated lake systems, none of these phases of lake level changes were ever documented in the volcanic area of the French Massif Central during the present interglacial period (Truze and Kelts 1993; Chapron et al. 2012; Lavrieux et al. 2013). Finally, the outlet of Pavin has been stabilized at an altitude of 1197 m only recently, by the building of human infrastructures at the end of the eighteenth century (Chap. 1, this issue).

One abrupt change of sedimentation pattern in core PAV10E occurring at ca. 20 cm below the lake floor on the subaquatic plateau (Fig. 23.2) has been related to a significant and rapid lake level drop (Chapron et al. 2012). The transition from in situ **diatomite** formation in the lower part of core PAV10E retrieved by 17 m water depth, into the deposition of a littoral facies just above an erosive sandy layer bearing some small sized organic macro remains (leaves debris) could not be dated by **AMS radiocarbon**. This change is interpreted as resulting from a lake level drop of ca. 9 m, considering that the deposition of the littoral facies in Lake Pavin occurs between the isobaths −26 m and the lake shore (Chap. 22, Fig. 23.1). Because excavation of the natural aerial outlet artificially dropped the level of Lake Pavin by ca. 4 m in the late eighteenth century (Chap. 1, this issue), these sedimentation changes in PAV10E can be related to an abrupt lake level drop of roughly 13 m.

Figure 23.9 compares DSR and RE pyrolysis measurements on cores PAV10E, PAV08 and PAV12. Following Debret et al. (2011), DSR data on a Q7/4 diagram suggest that either sediments from the littoral facies and in situ **diatomites** from these cores are organic-rich deposits dominated by Melonine type (B pole), by altered organic matter (C pole) and Chlorophyll and by-products (D pole). RE data represented by **S2** vs. TOC diagrams support DSR data and shows that Pavin sediments organic matter is always clustering within the algal pole. The organic matter from the littoral facies are, however, characterized by significantly lower values than in situ **diatomites** retrieved either in a littoral environment (PAV10E), on the plateau (PAV08) or in the basin (PAV12) of Lake Pavin. Interestingly, these diagrams also highlight that the upper **diatomite** unit from cores PAV08 and PAV12 are in addition characterized by lower values than the lower **diatomite** unit. This change in organic matter composition in Lake Pavin occurred just after the formation of the ca. AD 600 **slump** deposit on the subaquatic plateau (Figs. 23.4, 23.5 and 23.9) and can be explained by the progressive erosion and remobilization of oxidized littoral organic matter into the lake waters and its incorporation into the organic matter composition of the upper **diatomite** unit accumulated within the **mixolimnion** and the **monimolimnion** since this large mass wasting event. Such a progressive remobilization and incorporation of littoral organic matter within the upper **diatomite** after **sedimentary event** E6, suggest that this large **slump** deposit was contemporaneous to a major lake level drop of ca. 13 m at ca. AD 600.

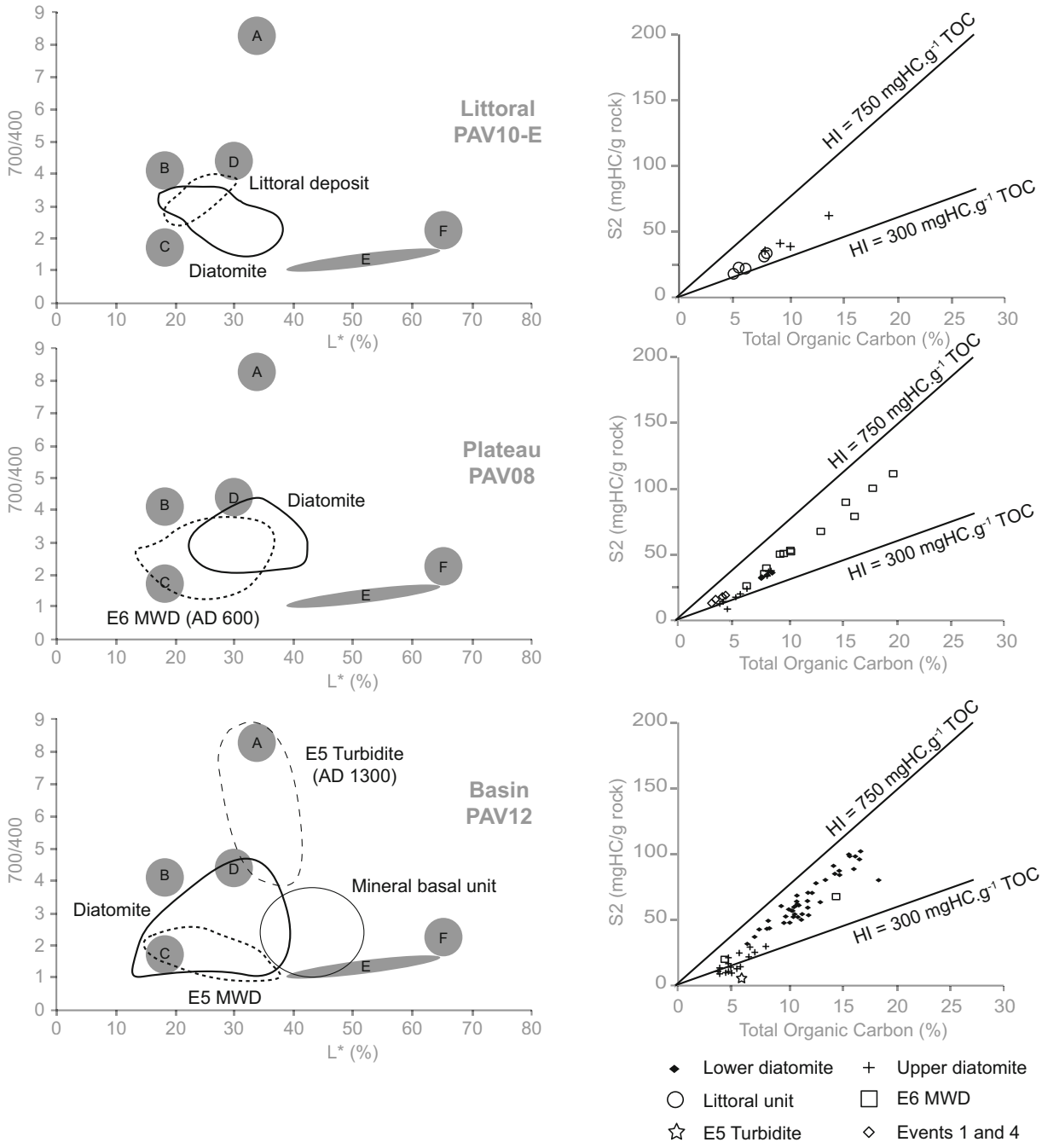

Fig. 23.9 Characterization of Pavin sediments origin and sediment source based on diffuse spectral reflectance Q7/4 diagram (*left*) and Rock-Eval pyrolysis represented by **S2** vs. TOC diagram (*right*) for cores PAV10-E (littoral), PAV08 (plateau) and PAV12 (basin). In the Q7/4 diagram, the diffuse spectral reflectance signature of littoral deposit, diatomite, Mass-Wasting Deposit (MWD), Turbidite and Mineral Basal unit are compared to the five distinct poles of sediments defined by Debret et al (2011): Iron-Rich deposits (**a**); Organic-rich deposits dominated Melanoidine type (**b**); Organic-rich deposits dominated by altered organic matter (**c**); Organic-rich deposits dominated by Chlorophyll and by-products (**d**); Clayey deposits (**e**) and Carbonate deposits (**f**). In the **S2** vs. TOC diagram, Total Organic Carbon (TOC), together with Hydrogen Index (HI) and **S2** (thermal cracking of the hydrocarbon compounds) are illustrated. The two linear domains of the hydrogen index (HI = 750 and HI = 300 mgHCg^{-1}TOC) corresponding to algal and terrestrial poles, respectively, are also represented

23.4.2 Evolution of Pavin Limnology

In some anoxic subaquatic environments, b* parameter measured on sediment cores has been used to track the evolution of diatoms content (Debret et al. 2006, 2011) and used as a proxy to document the evolution of the productivity of aquatic environments. As shown in Fig. 23.8, in Lake Pavin, b* parameter is, however, clearly different from the evolution of Si/Ti ratio measured by XRF core scanning and used here as an indicator of diatom production. It suggests that b* parameter can't be used here to document the evolution of its productivity. Lake Pavin sequence highlights a progressive and fluctuating increase in Si/Ti since 7000 cal BP culminating around 5000 cal BP, but this ratio is later on slightly reduced since 4200 cal BP and remained much more constant afterwards. This trend suggests that Lake Pavin productivity has been more variable and intense in the early Holocene and then stabilized during the mid-Holocene. Interestingly, TOC in PAV12 sediments shows a slightly different evolution through time, with a progressive increase since 7000 cal BP culminating around 3500 cal BP, and a decreasing trend afterwards. This bimodal evolution is, however, not observed in HI values that are quickly rising within the basal mineral unit and then remaining relatively constant within the lower **diatomite** unit, before sharply dropping in the upper **diatomite** unit. Such a complex evolution of organic sedimentation in Lake Pavin suggests that this crater lake underwent several steps and important changes in its productivity and in the preservation of organic matter on its floor.

Following Albéric et al. (2013), the confrontation between **AMS radiocarbon** dates obtained from bulk sediments and either leaves debris sampled at similar depths or corresponding model ages in the lower **diatomite** unit from core PAV12 (Table 23.1, Fig. 23.6), is, in addition, suggesting the development of a significant **radiocarbon reservoir effect** ranging around 2500 yrs at ca. 8 m core depth (i.e. near 3000 cal BP) and up to ca. 3800 yrs near 6.5 m core depth (i.e. around 1700 cal BP). These new data have been added in Fig. 23.10, adapted from Albéric et al. (2013), where radiocarbon reservoir effect (either in ^{14}C age scale or $\Delta^{14}C$ scale) is plotted versus calibrated model ages of Lake Pavin sediments. Although the link between the meromicticity and the existence of large reservoir effects is not univocal (Albéric et al. 2013), this suggests that the **meromicticity** of Lake Pavin started early in the lake history and may have been variable through time.

Lake Pavin **meromicticity** is also known to impact the geochemistry and biogeochemical cycles in the deep central basin (Part III, this issue) and favoring the storage of dissolved Fe (by the so-called iron-well process (Martin 1985)) and Mn in sediments from the **monimolimnion** (Viollier et al. 1995; Jezequel et al. 2011; Schettler et al 2007). A clear increase in Fe/Mn ratio within the upper **diatomite** unit in

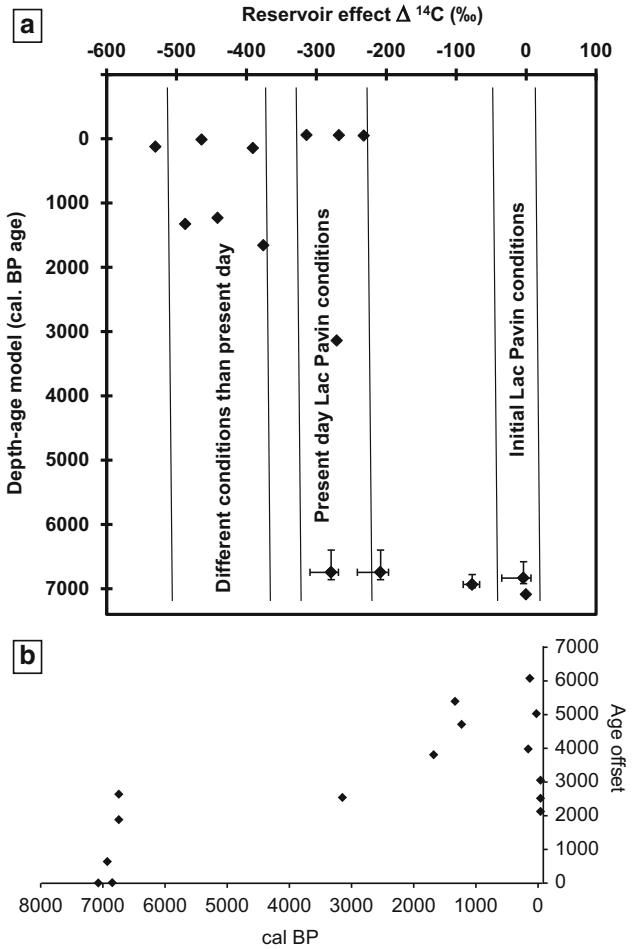

Fig. 23.10 Radiocarbon reservoir effect (**a**) and age offset (**b**) evolution since Lake Pavin formation (Modified after Albéric et al. (2013)

PAV12 (Figs. 23.5 and 23.8) may thus partly reflect an intensification of the **meromicticity** after sedimentary event E5. These XRF measurements were, however, performed several weeks after core sections opening, and it seems also very likely that such a significant increase in Fe/Mn ratio in the upper **diatomite** unit is partly an artefact link with an intense oxidation of PAV12 sediment interstitial water. SDR measurements on PAV12 were, on the contrary, performed just after core sections opening on "fresh" sediments and may thus be more reliable to track the evolution of iron oxides in Pavin sediments. Interestingly, the evolution of the first derivative values at 525 and 445 nm, corresponding to the occurrence of goethite in the sediments (Debret et al. 2011; Simonneau et al. 2013b), is highlighting a major increase in the lower **diatomite** unit ca. 2700 yrs ago (Fig. 23.8). As a working hypothesis, it seems therefore likely that the **meromicticity** of Lake Pavin developed during the late Holocene period, rather than just after the crater formation.

Ongoing investigations on the evolutions of diatoms assemblages in PAV12 sediments can bring important additional arguments to reconstruct changes in lacustrine

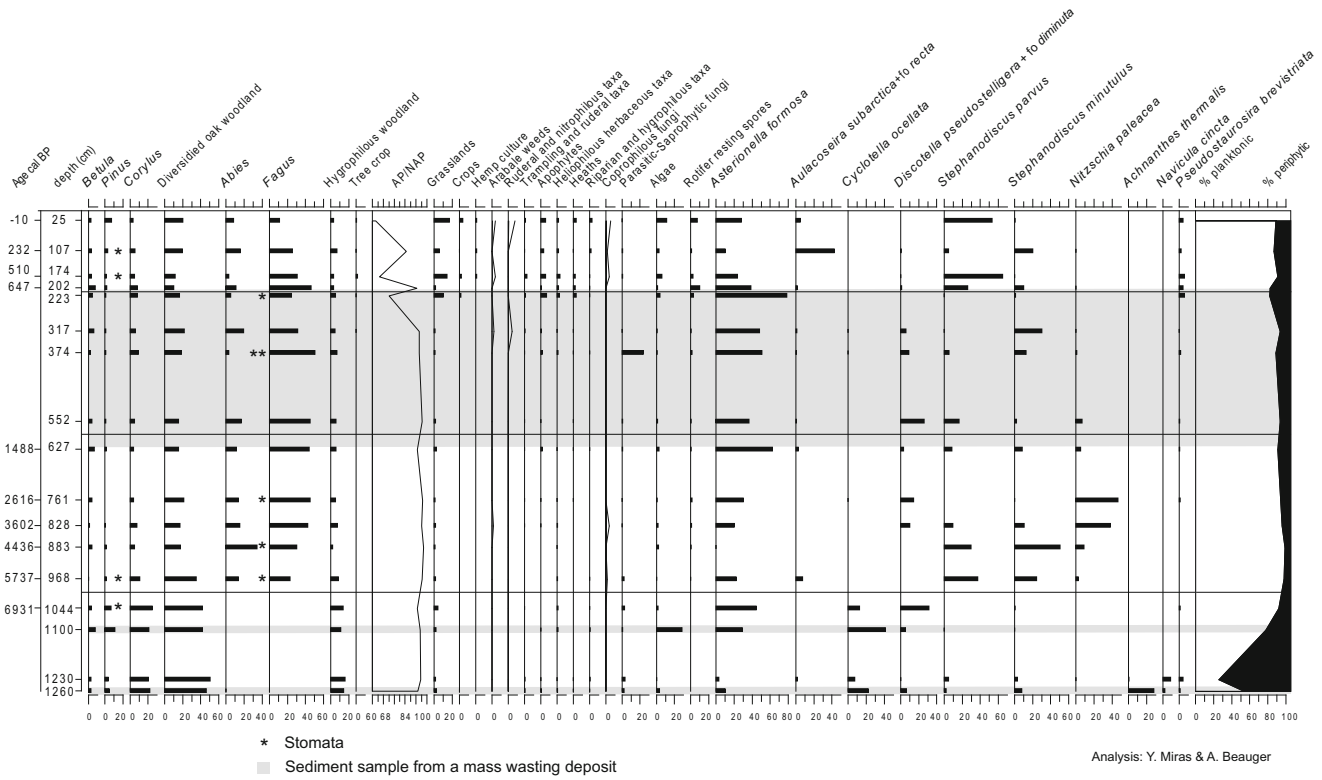

Fig. 23.11 Preliminary pollen (*left*) and diatom (*right*) diagram illustrating the evolution of species assemblages in sediment from PAV12 sampled either in reworked deposits (i.e. turbidite or mass wasting deposit; grey levels) and *in situ* deposits. The ratio from arboreal and none-arboreal pollen (AP/NAP) is also given

dynamic. Figure 23.11 shows preliminary results of analysis performed either within *in situ* laminated lacustrine sediments or within mass wasting deposits. Such a strategy can provide insights on environmental changes and on sediment source areas in remolded deposits, as discussed below. In the basal unit around 7000 cal BP, the diatom community during this period are either typical from alkaline and electrolyte rich waters (*Achnanthes thermalis* (Rabenhorst), Schoenfled var. *thermalis, Fragilaria famelica* (Kützing) Lange-Bertalot var. *fameilica* and *Navicula cincta* (Her.) Ralfs), littoral taxa (*Staurosirella pinnata* Ehrenberg, *Staurosira venter* (Ehr.) Cleve & Möller) or epithytic taxa (*Epithemia* spp, *Cocconeis* spp, *Rhopalodia gibba* (Her.) O. Muller) associated with the development of macrophytes (Walker and Paterson 1986; Van Dam 1994; Lange-Bertalot 2001; Hindakova 2009; Gutowski et al 2011). Opportunistic diatom species (*C. ocellata*) together with *Botryococcus* algal spores are in addition typical from deep and oligotrophic lakes (Blomqvist et al. 2001; Rioual et al. 2007). These assemblages suggest that Lake Pavin became a deep and oligotrophic lacustrine system quickly after the Pavin eruption. The presence of littoral diatom taxa in the deep central basin within laminated clastic sediments and within **turbidites** can also be explained by the development of numerous active canyons incised into the Pavin crater formation: these features are still visible in the morphology along the steep slopes of the lake (Fig. 22.10) and could easily bypassed material in the past from surrounding sub aerial and littoral environments to the deep water basin. In the lower **diatomite** unit, non-pollen palynomorphs assemblages mainly dominated by algal spores (*Debarya* and *Spyrogyra*), together with the development of spring diatom bloomers (different species of *Stephanodiscus*) and a change in rotifer resting eggs (*Conochilus hippocrepis*-type is progressively replaced by *Keratella*-type, *Filinia longiseta*-type and *Brachionus*-type) are suggesting an increasing trend in the trophic state of the lake (Lotter and Bigler 2000; Barbiero and Warren 2011). After 2600 cal BP, there is a replacement of *Stephanodiscus* by different planktonic genuses, with the dominance of *Nitzschia paleacea* (*Grunow*) indicating higher concentration of NH4 in the lake (Voigt et al. 2008). Interestingly, a peak in Ti (Figs. 23.5, 23.8 and 23.12) is observed during this time window and such trophic change could be explained by sediment inputs in the lake, but further studies (and higher resolution samples of diatoms assemblages) are needed to confirm this assumption. The disappearance of littoral taxa within this lower **diatomite** unit, suggest a limited influence of canyons. This is apparently also true for the upper **diatomite** unit. In the latter unit, dominant taxa (*A.formosa* and different species of *Stephanodiscus*) are typical from nutrient-rich waters. The

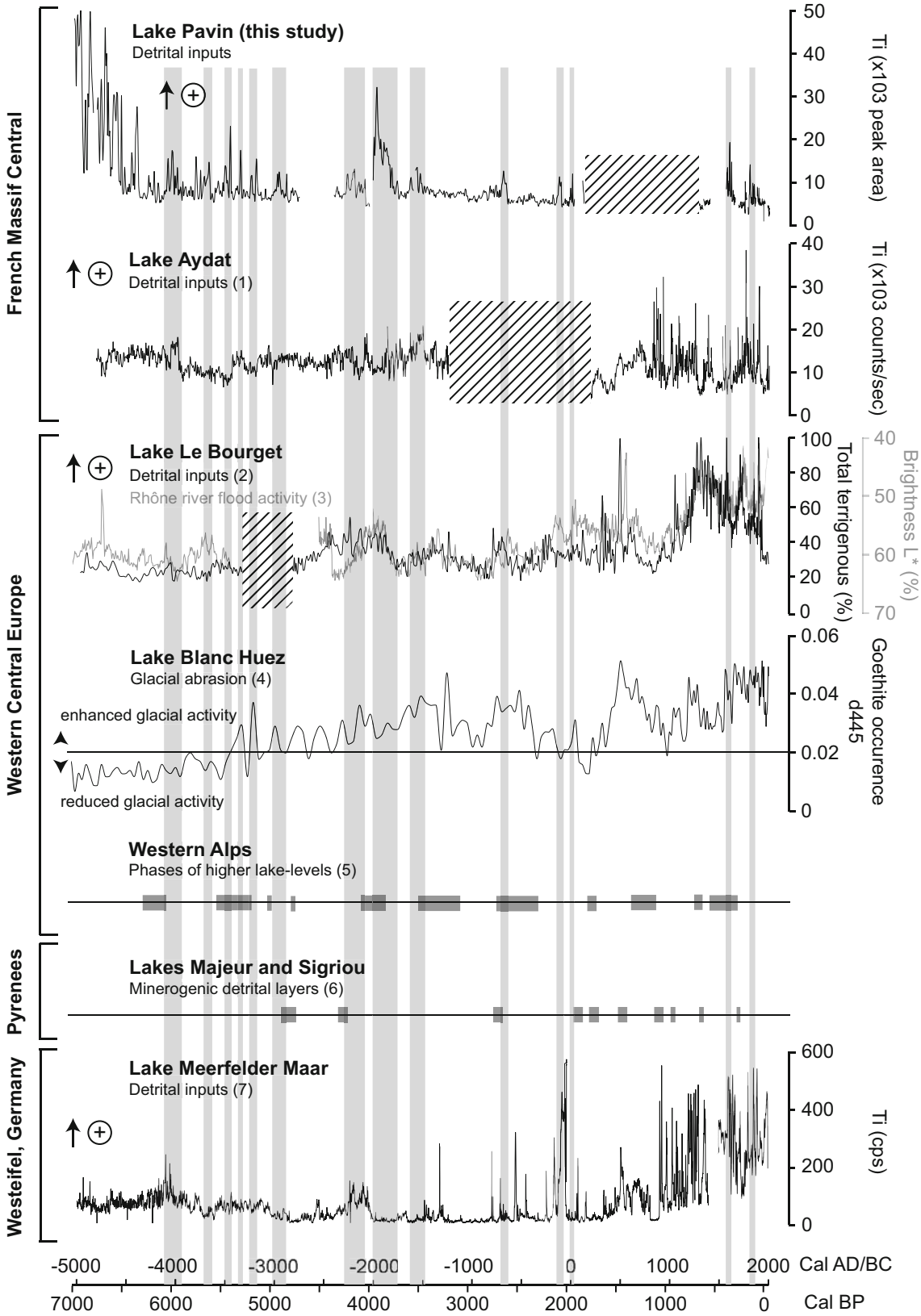

Fig. 23.12 Comparison of detrital inputs in Lake Pavin with other records in Western Europe (1) Lavrieux et al. (2013); (2) Arnaud et al. (2012); (3) Debret et al. (2010); (4) Simonneau et al. (2014); (5) Magny (2006); (6) Simonneau et al. (2013b); (7) Martin-Puertas et al. (2012). *Grey squares* represent phases of enhanced terrestrial supplies in Lake Pavin (this study). Hatched areas correspond to unrecorded periods due to Mass-Wasting Deposits

dominance of *Aulacoseira subarctica* (O. Muller) Haworth ca. 200 years ago in association with higher frequencies of small periphytic *Fragilaria*, *Staurosira* together with the decrease in diatoms and chrysophyceae cysts densities suggest, however, the development of a colder period and a change in the trophic status (Van Dam 1994).

23.5 Impact of Climate, Human and Geological Hazards on Lake Pavin Sedimentation

Ongoing investigations on the evolutions of pollen assemblages in PAV12 sediments are also given in Fig. 23.11 and are reflecting either local or regional changes in the vegetation cover. Together with independent indicators of terrestrial inputs to Lake Pavin, pollen data may help to disentangle environmental changes induced by climate and human activities. As discussed below, pollen and diatom assemblages from mass wasting deposits in core PAV12, can in addition provide insights on sediment source areas and further support stratigraphic and chronological reconstructions to precise the impact of geological hazards on Lake Pavin sedimentation.

In between the **turbidites** from the basal unit around 7000 cal BP, pollen data clearly indicate the occurrence of a diversified deciduous forest dominated by oak (*Quercus*) and also filled by lime tree (*Tilia*), elm (*Ulmus*), maple (*Acer*) and ash (*Fraxinus*). This forest dominated the regional landscape during the Atlantic period (Reille et al. 1992) and the pollen frequencies reached in PAV12 samples suggest that this vegetation was very close to Lake Pavin. The identification of alder (*Alnus*), birch (*Betula*), Hazel (*Corylus*) and pine (*Pinus*) and also of pine stomata further indicate that the slopes of the carter rim of Lake Pavin were quickly colonized by plants. Maximum values of Ti in this basal unit (Figs. 23.5 and 23.12) and the occurrence of coarse-grained **turbidites** suggest, however, a limited vegetation cover within the inner slopes of the **crater rim** and a significant erodability of (subaerial and subaquatic) slopes draining into the lake. It seems thus likely that plant colonization along the inner slopes of the **crater rim** came from the crest of the rim. In addition, in this early stage of Lake Pavin, it is likely that the lake surface was much higher than today and closer to crest of the rim.

In the lower **diatomite** unit, the development and maturity of beech (*Fagus*) and fir (*Abies*) woodlands matches the regional climatic variation of the Mid-Holocene toward wetter and cooler conditions (Magny and Hass 2004; Lavrieux et al. 2013). Such conditions also favored the development of vegetation on the shore of Lake Pavin dominated by alder. Regular occurrences of fir stomata and parasitic and saprophytic fungi of tree (Cugny et al. 2010) underline the presence of fir and other caducifolious tree species. These reconstructions indicate that the inner slopes of the crater were densely covered by vegetation and are in agreement with the observed limited clastic sediment supply reflected (i) by low Ti content within this lower **diatomite** unit and (ii) by increasing concentration of algal organic matter. Since the onset of this organic rich sedimentary unit, the erodability of subaerial slopes draining into the lake was thus much probably reduced. The identification of several peaks in Ti within the lower **diatomite** unit (Figs. 23.5, 23.8 and 23.12) suggest, however, that short periods of enhanced erosion occurred within the drainage basin of Lake Pavin. Because some of these erosive periods at Lake Pavin are also matching periods of enhanced clastic inputs in nearby Lake Aydat (Fig. 23.1), but also in more remote lakes from the western Alps (lakes Bourget and Blanc Huez), the northern Pyrenees (lakes Majeur and Sigriou) and eventually in the Eiffel volcanic province in Germany (maar lake Meerfelder) as shown in Fig. 23.12, they might reflect larger scale climate shifts. Phases of enhanced precipitation at the onset of the Neoglacial period (between 6000 and 5000 cal BP), during the Bronze Age (between 4300 and 3500 cal BP), at the beginning of the Iron Age (between 2800 and 2600 cal BP) and during the Roman period (around 2000 cal BP) in Lake Pavin might for example match periods of enhanced soil erosion in Lake Aydat (Lavrieux et al. 2013), higher Rhone River flooding activity in Lake Le Bourget (Debret et al. 2010; Arnaud et al. 2012), increasing glacier activity in Lake Banc Huez (Simonneau et al. 2014), phases of higher lake-levels in the Western Europe (Magny 2006; Magny et al. 2013), reactivation of canyons draining into lakes Majeur and Sigriou (Simonneau et al. 2013b) and soil erosion in maar lake Meerfelder (Martin-Puertas et al. 2012). These clastic input peaks in Lake Pavin could either result from the direct impact of periods of heavy rainfalls on runoff along the steep slopes of the **crater rim** characterized by numerous gullies and thalwegs (Fig. 22.10) or from enhanced soil erosion favored by the effect of snow amount on runoff during periods of snowmelt (Tanasienko et al. 2011; Simonneau et al. 2013b).

In the upper **diatomite** unit, a radical change in the regional landscape is depicted by pollen data. The woodland cover present a significant decreasing trend while grasslands and heathlands increase as illustrated by the ratio between arboreal and none arboreal pollen concentrations (AP/NAP) shown in Fig. 23.11. During this period, Stebich et al. (2005) also describe a more open landscape and pollen assemblages typically resulting from the development of grazing, crops and hemp cultures. In core PAV12, apophytes, trampling and ruderal pollen indicators together dung-related fungal spores (e.g. *Sporormiella* and *Coniochaeta lignaria*) indicate grazing activities throughout the zone and as well as the predominance of the rotifer assemblage (*Conochilus natans*) suggest

a change in the lake water conditions. The vegetation of the lake shore constits of a sedge community and both lower arboreal pollen frequencies and the disappearance of tree stomata could suggest that woodlands are not so extended in the lake shore than previously. It is, however, important to keep in mind that Lake Pavin watershed is larger than its topographic drainage basin due to the occurrence of numerous subaerial and subaquatic springs (Fig. 22.1, Chap. 22). The precise limits of Pavin watershed are still poorly defined, but it has been shown that nowadays the lake water trophic level is highly sensitive to agricultural practices outside the crater rim (Chap. 1). It seems thus very likely that this has been the same in the past. Accordingly, the development over the last seven centuries of agricultural practices outside the **crater rim** probably impacted land use (and thus pollen rain at a regional scale) but also the trophic level of Lake Pavin (and thus diatom assemblages or non-pollen palynomorphs such as rotifer resting eggs). This interpretation is in agreement with old paintings from Lecoq realized in AD 1867 discussed in Chapron et al. (2010) and illustrating a former Lake Pavin panorama dominated by grasslands outside the **crater rim**, while its inner slopes (i.e., the topographic drainage basin of Lake Pavin) were still largely forested. Only two peaks in Ti are in addition observed in the upper **diatomite** unit in PAV12, while lakes Aydat, Bourget and Meerfelder are clearly characterized by increasing trends in detrital inputs over the last two millennia (Fig. 23.12). These trends of detrital inputs in these contrasted European lacustrine systems were related to increasing soil erosion due to development of land use and agriculture in their watersheds (Lavrieux et al. 2013; Debret et al. 2010; Arnaud et al. 2012 and Martin-Puertas et al. 2012). Because these two peaks in Ti are occurring during the Little Ice Age (LIA) in PAV12 and are contemporaneous with periods of enhanced flooding activity in lakes Aydat and Bourget (Lavrieux et al. 2013; Arnaud et al. 2012; Chapron et al. 2005), but also glacial activity in the Alps (Arnaud et al. 2012; Simonneau et al. 2014) and soil erosion in maar lake Meerfeler (Martin-Puertas et al. 2012), they are probably more reflecting a climatic signal (shits toward colder and wetter conditions) than anthropic activities. Following these authors (and numerous studies in Europe), it is, however, very likely that human practices during the LIA, had impacts on the watersheds vegetation cover and favored detrital inputs to these lakes, including in Lake Pavin.

Clear traces of recent human activities in the Pavin topographic drainage basin are sparse and concern essentially the building of successive infrastructures to stabilize its outlet (Chap. 1) and the development of some tracks and paths along the inner slopes of the **crater rim** (Fig. 22.10). To some extent, it is very likely that woodlands around Lake Pavin were used for domestic needs over the last centuries, but this maar lake might be in fact considered as one of the few preserved natural site in the French Massif Central. As further discussed in Chaps. 1, 2 and 3 this specificity of Lake Pavin in the region may be more related to its "dangerous" reputation than its relatively limited accessibility. In this paper and in Chap. 22, several stratigraphic and geomorphologic evidences are also highlighting the development of a wide range of subaquatic slope instabilities and at least two large events associated with the generation of violent waves since the lake formed ca. 7000 years ago (Chapron et al. 2012). It seems therefore possible that geological hazards in this maar lake may have contributed to its preservation from growing human activities over the last millennia.

Sedimentary event labeled E1 presented in Chap. 22 is only identified on the plateau at site PAV08 (Fig. 22.8). This 2 cm thick light colored layer (higher L* values) is characterized by lower TOC and HI values bearing a similar organic matter signature on a **S2** vs. TOC diagram than littoral sediments as shown in Fig. 23.9. According to the new age-depth model established for PAV08-P1 (Fig. 23.4), this **sedimentary event** E1 is dated to AD 1915 +/− 5 and can be correlated with the historical earthquake that stroke the town of La Bourboule in AD 1921 located at only 15 km from Lake Pavin (Fig. 23.13; Table 23.2). This earthquake reached an MSK intensity of 4.5 at the epicenter (Sisfrance database, BRGM, Lambert 1997). Compared to other studies documenting the impact of historical earthquakes on lacustrine sediments from European regions characterized by a moderate seismicity (Chapron et al. 1999; Monecke et al. 2004; Nomade et al. 2005; Strasser and Anselmetti 2008), it seems that Lake Pavin organic rich sedimentation in littoral areas is unstable and easily remobilized when submitted to gravity accelerations associated with seismic waves propagation. Following the conclusions of Strasser and Anselmetti (2008) it is, however, also very likely that this limited remobilization of littoral sediments down to PAV08 coring site has been favored by the perturbation of subaqueous sediment pore pressure after the artificial lake level drop by ca. 4 m in the late eighteenth century (Chap. 1, this issue). **Sedimentary event** labeled E2 described in Chap. 22 is only identified at a single site from the deep central basin in core PAV09-B1 (Fig. 22.8). This 2 cm thick layer is essentially characterized by very high values in MS and is dated to AD 1880 +/− 70. Given the dating uncertainties, this event interpreted has a fine grained **turbidite** originating from a canyon, is potentially contemporaneous with two nearby historical earthquakes that stroke the study area in AD 1863 (the Mont-Dore MSK intensity 5 event) and in AD 1892 (the Issoire MSK intensity 7 event) located at 11 km and 29 km from Lake Pavin, respectively (Fig. 23.13; Table 23.2). According to former studies on lacustrine sediments sensitivities to instrumental earthquakes (Monecke et al. 2004; Nomade et al. 2005) both of these historical earthquakes could be recorded in nearby Lake Pavin. Another similar study combining

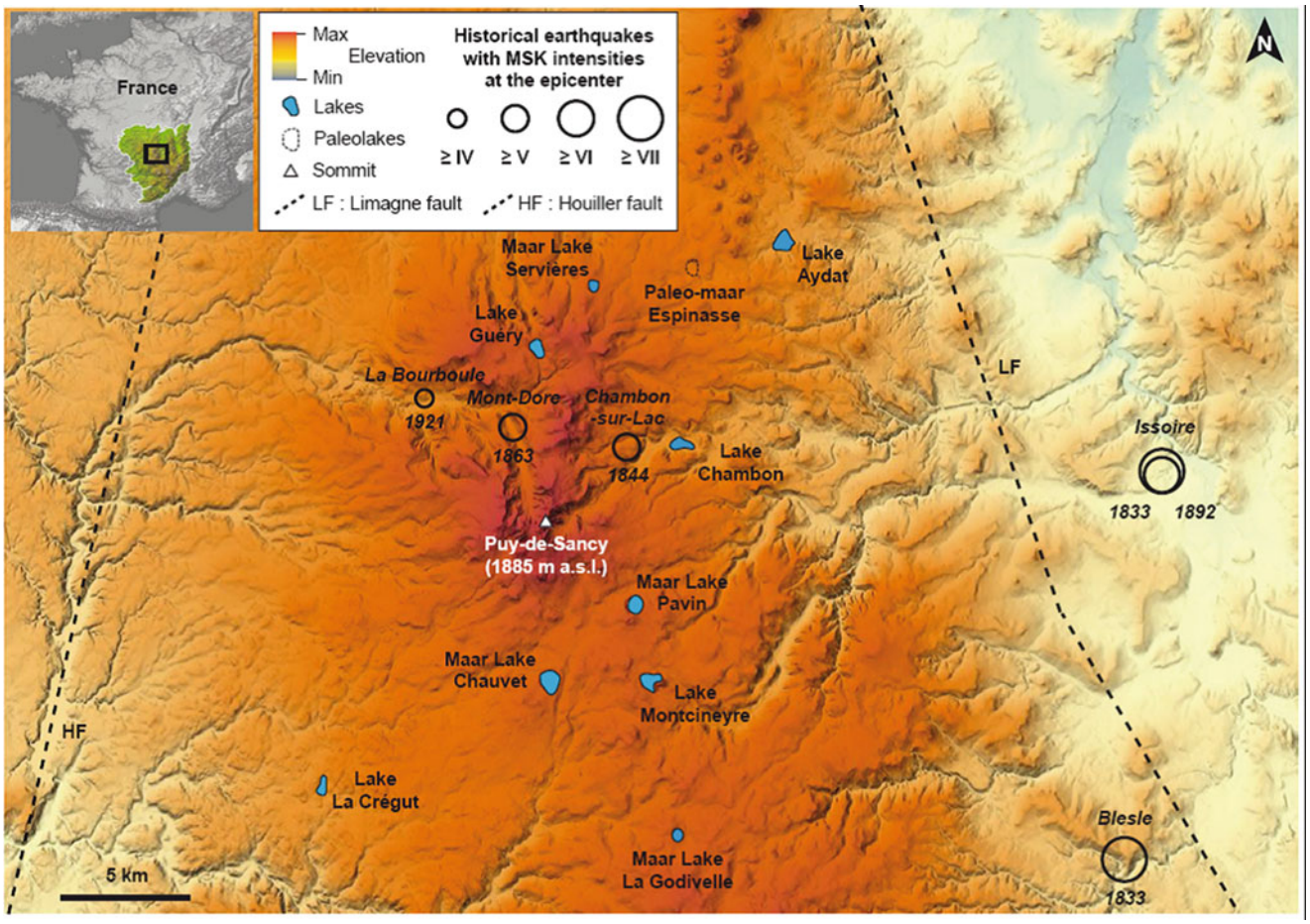

Fig. 23.13 Digital elevation model of the Northern part of the French Massif Central illustrating the location of lacustrine systems and MSK intensities of historical earthquake epicenters that stroke the study area. Regional faults (the Limagne Fault, LF and the Houiller Fault, HF) are also indicated by *dashed bold* lines

radiocarbon dated sediment cores from nearby Lake Guéry (Chassiot et al. 2016) also identified a pluri-decimetric **slump** deposit along its delta that is contemporaneous with the AD 1863 Mont-Dore earthquake (Fig. 23.13). As shown in the above mentioned former studies, regional contemporaneous slope instabilities in lacustrine environments are one of the stronger arguments to link a mass wasting deposit (MWD) with earthquake shaking. Another crucial criteria being that the age of the MWD fits with an historical earthquake. It seems thus likely that E2 in the Pavin central basin resulted from earthquake shaking in AD 1863. To support this interpretation, ongoing studies on this **sedimentary event** involve grain size and RE measurements, in order to document possible sediment source areas and to explain high magnetic susceptibility values in E2. Similarly, **sedimentary event** labeled E3 only documented in core PAV09B1 by MS measurements (Fig. 22.8) and dated to AD 1840 +/− 80, is potentially contemporaneous with two others nearby historical earthquakes that stroke the study area in AD 1844 (the Chambon-sur-lac MSK intensity 5.5 event) and in AD 1833 (the Issoire MSK intensity 6 event) located at 9 km and 29 km from Lake Pavin, respectively (Fig. 23.13; Table 23.2).

As shown in Fig. 22.8 and Table 23.2, **sedimentary event** labeled E4 is identified both on the plateau (PAV08-P1) and in the deep central basin (PAV09-B1). Clustering calculated ages for these two contrasted layers allow correlating them with a single event that occurred likely between AD 1685 and 1715, and eventually later (i.e. between AD 1685 and 1865 according to dating uncertainties on core PAV09-B1), since E4 on the plateau has an erosive base, and may thus be complicated to date as shown in Fig. 23.4. On the plateau, this 6.5 cm thick light colored layer, is like E1, containing organic matter originating from the littoral environments (Fig. 23.9). One **AMS radiocarbon age** within E4 on the plateau suggest, in addition, that remolded littoral sediments are significantly older than the event. In the deep central basin, E4 is thinner than sedimentary events E2 and E3, but characterized by a maximum value in MS and a clear change is SDR values (compared to the host sediment) that is similar

to the one found for E4 on the plateau (Fig. 22.8). It seems thus here very likely that sedimentary E4 consist in reworked former littoral sediments developing a thin mass wasting deposit that froze on the plateau at PAV08 coring site, but evolved down slope into a thin and fine grained **turbidite** at PAV09B1 coring site. Due to age uncertainties, this sedimentary event may be related to perturbation of subaqueous littoral sediment pore pressure after the artificial lake level drop by ca. 4 m in the late eighteenth century (Chap. 1, this issue) and thus be human induced. It may also be linked to a former **limnic eruption** described back to AD 1783 in the so-called Godivel IV manuscript detailed by Michel Meybeck in Chap. 2 (this issue). The translation of this old manuscript suggest that the August 21, 1783 event was a "moderate degassing [event] due to lake rollover" eventually in relation with internal slumping according to Meybeck and potentially associated with two historical earthquakes (Table 23.2) of unknown MSK intensities and epicenter locations but documented in the Limousin region in the French historical earthquake catalogue Sisfrance (i) the same day (the Lepaud event) and (ii) in July (unknown precise date) that same year in a similar location (the Mainsat event). Further palaeoseismological studies are however required to better document the potential impact of these earthquakes in the study area.

Sedimentary event labeled E5 is a major **slump** deposit capped by a muddy **turbidite** found both in cores PAV99 (510 cm thick) and PAV12 (420 cm thick) in the deep central basin of Lake Pavin (Fig. 23.2; Table 23.2) and dated to AD 1282 +/− 20 according to the PAV12 age-depth model (Fig. 23.6). This major mass wasting deposit originates from a fresh **slide scar** at the edge of the plateau (Fig. 23.3) and is correlated with a slightly older but outstanding erosive sandy layer bearing organic macro remains dated to AD 1190 +/− 30 at coring site PAV09-C5 in the littoral environment identified north of the plateau (Fig. 23.2). This interpretation suggesting that this large **slide** was associated with violent and erosive waves along the lake shore is in agreement with available sedimentary facies, stratigraphy, SDR and RE data (Fig. 23.9). Firstly, only rare large waves could form an outstanding erosive sandy layer in littoral core PAV09-C5 and rework coarse littoral particles with numerous leaves debris. Secondly, the leave debris dated by **AMS radiocarbon** in this coarse layer can be older than the event. Thirdly, in a Q7/4 diagram, the E5 MWD in PAV12 is mainly made of **diatomite** material accumulated on the plateau (i.e. similar to the **diatomite** found in the lower unit of PAV10-E), while E5 **turbidite** as a different signature. Finally, in a **S2** vs. TOC diagram, the E5 MWD has a similar organic composition than the lower **diatomite** unit, but E5 **turbidite** contains mainly terrestrial organic matter. It seems thus likely that large and erosive waves triggered by the slide of **diatomite** could export down to the central basin some of the fine grained material deposited within the E5 **turbidite**, while E5 MWD was already frozen at the basin floor. Pollen data are showing variable percentages of assemblages dominated by arboreal pollen (mainly beech, oak, fir and hazel) within the base of E5 MWD, with a sudden drop of beech percentages synchronous with first record of tree crops like chestnut (*Castanea*) and walnut (*Juglans*) in the upper part of E5 MWD. Such results are in agreement with available **radiocarbon ages** in PAV99 within this deposit and are both suggesting sediment remolding and loss of chronological order within the **slump**. In the E5 **turbidite**, numerous parasitic and saprophytic fungal spore of hydrophilous vegetation and the noticeable presence of fir stomata are originating from the lakeshore and this pattern may have been favored by wave propagation along the lakeshore. Diatom assemblages in E5 MWD consist in a mix of different planktonic species from the pelagic zone (*A.formosa*, different species of *Stephanodiscus*), associated with diverse Fragilariaceae-benthic assemblage, as *Staurosira construens* known to live in the littoral zone. Once again, there is a change in E5 **turbidite** where different indicators (rotifer like *Brachionus* or cyanobacteria such as *Aphanizomenon* and diatom as *Eolimna minima*) suggest higher trophic level (Barbiero and Warren 2011). Consequently, it is thus likely that E5 **turbidite** had a slightly different sediment source than E5 MWD, due to the generation of violent waves along the lakeshore.

In a previousstudy, Chapron et al. (2012) suspected earthquake triggering for this large event E5 in Pavin, since it seems contemporaneous to a remarkable **slide** in nearby Lake Montcineyre (Fig. 23.13). This is further supported now by available **radiocarbon** dating in Lake Montcineyre dating this **slide** around AD 1320 +/− 10) and by the dating of another contemporaneous MWD back to cal. AD 1310 +/− 100 in Lake Guéry located in the Puy de Sancy area, ca. 7 km north from Pavin (Chassiot et al. 2016). Ongoing radiocarbon dating will tell if a third regional MWD in Lake La Crégut (at ca. 20 km from Pavin) and the outstanding slump and turbidite deposits in maar Lake Chauvet described in Chap. 22 (this issue), are also contemporaneous. As shown in Table 23.2, **sedimentary event** E5 may also be contemporaneous to a reported earthquake in the Limousin region in June, 13 AD 1348 (the Uzerche event of unknown both intensity and precise epicenter location). Since this event occurred few decades after the calculated age of E5 based on PAV12 chronology, it means that additional dating uncertainties in PAV12 age-depth model within the upper **diatomite** unit maybe related with unidentified sediment erosion episodes associated with the development of **turbididty currents** that deposited sedimentary events E2, E3 and E4 at site PAV09-B1.

A set of new data from **sedimentary event** E6 presented in this study, allows to further precise the sediment source areas and the consequences of this other major event that deeply impacted Lake Pavin (Chapron et al. 2010, 2012).

The changes in organic matter geochemistry observed just after this event (enrichment of organic matter of terrestrial origin or oxidized organic matter in the upper **diatomite** unit in both PAV8 and PAV12 coring sites) and related to the progressive erosion and remobilization of exposed former littoral lacustrine sediments following an abrupt lake level drop of ca. 13 m, suggest (i) that E6 MWD was much probably favored by the perturbation of subaqueous sediment pore pressure during the lake level drop and (ii) that this large MWD on the plateau was therefore associated with a major **lake outburst** and a catastrophic debris flow downstream in the Couze Pavin valley. As shown in Table 23.2, a similar age obtained from the second outstanding erosive sandy layer at site PAV09-C5, further points toward the propagation of violent waves during this event. The origin of the **lake outburst** is, however, still unknown. It may either result from a wetter period since there is a general increase in detrital sediment supply to regional lacustrine systems around AD 600 in Western Europe (Fig. 23.12), but it may also result from earthquake shaking, since several younger seismic events were apparently recorded in this maar lake by slope failures. Finally, as discussed in Chap. 3 (this issue), this major environmental crisis at Lake Pavin and downstream in the Pavin valley ca. 1400 years ago, may have cause the end of a Roman query at the shore of Lake Pavin documented in a text from Gregorius of Tours, one of the first historian of Gaul relating pagan lake cults and regular catastrophic events in Auvergne (Chap 2, this issue). It is however beyond the scope of this paper to further discuss the possible evolution of human activities within the topographic drainage basin of Lake Pavin since the Roman period, because this time window is not documented in core PAV12 due to sediment erosion at the base of sedimentary event E6.

23.6 Conclusions and Perspectives

The multidisciplinary study of Lake Pavin sedimentary infill combining acoustic soundings, and well-dated sediment cores together with the integration of regional and historical data sets on climate, human activities and natural hazards in the study area highlight that:

(i) Lake Pavin sedimentation was essentially dominated by mineral inputs from the drainage basin following the formation of Pavin crater;
(ii) Afterwards, the rapid development of vegetation cover along the inner slopes of the crater limited strongly mineral inputs toward the lake and favored the formation of **diatomite**, an organic rich sedimentation dominated by the productivity in the water column over the last ca. 7000 years;
(iii) The identification of several short periods of enhanced mineral inputs within the diatomite deposits contemporaneous with similar trends observed previously in contrasted lacustrine systems from western Europe, might reflect the influence of climate change (i.e. wetter periods) on Pavin sedimentation;
(iv) The development of Pavin **meromicticity** may have been favored by the occurrence of at least two major subaqueous slope failures dated at ca. AD 600 and ca. AD 1300. These two events were associated with unusual erosive waves at the lake shore and related with a catastrophic **lake outburst** and a lake level drop of ca. 13 m some 1400 years ago and regional earthquake shaking some 700 years ago, respectively;
(v) Apparently limited human impact on Pavin sedimentation since the Roman period is unusual in this region and may result from the catastrophic consequences of large subaquatic slides around AD 600 and AD 1300, but also recurrent more limited slopes failures since the Little Ice Age possibly triggered by regional historical earthquakes (in AD 1783; in either AD 1833 or AD 1844; in AD 1863 and in AD 1921) and eventually associated with a **limnic eruption** in AD 1783. Further studies integrating archeology, paleo ecology and lacustrine sedimentology are still needed to better document the impact of former societies on the environment in the study area. Enhanced slope instabilities since the end of the eighteenth century may, however, resulted from the perturbation of subaqueous sediment pore pressure after the artificial lake level drop by ca. 4 m.

Future and ongoing studies on Lake Pavin area should confirm the timing, causes and consequences of this event stratigraphy based on similar limnogeological approaches in several contrasted regional lakes, in order to further pinpoint the respective influences of climate changes and land use evolution on lacustrine sedimentation. Finally, this reconstruction of Lake Pavin paleolimnology and event stratigraphy should help reconstructing the history of its **meromicticity** and the evolution of its remarkable biodiversity.

Acknowledgements This study benefited from several projects funded by (i) the MEEDDAT project of the DDEA Puy-de- Dôme, (ii) the Agence de l'Eau Loire-Bretagne (AELB) project EDIFIS, (iii) the INSU project DICENTIM and (iv) the ARTEMIS facilities from INSU and INSHS for radiocarbon dating. L. Chassiot PhD grant is in addition funded by the Région Centre. We wish to thank Anaëlle Simonneau (ISTO, Orléans) for field work support and scientific discussions, Alice Recanati (LMCM, Paris) for MEB pictures and Michel Meybeck for scientific discussions. We wish to thank Prof. Marc Desmet for his constructive review of this chapter.

References

Aeschbach-Hertig W, Hofer M, Kipfer R, Imboden DM, Wieler R (1999) Accumulation of mantle gases in a permanently stratified volcanic lake (Lac Pavin, France). Geochim Cosmochim Acta 63(19–20):3357–3372

Albéric P, Jézéquel D, Bergonzini L, Chapron E, Viollier E, Massault M, Michard G (2013) Carbon cycling and organic radiocarbon reservoir effect in a meromictic crater lake (lac Pavin, Puy-de-Dôme, France). Radiocarbon 55(2–3):1029–1043

Ariztegui D, Chondrogianni C, Lami A, Guilizzoni P, Lafargue E (2001) Lacustrine organic matter and the Holocene paleoenvironmental record of Lake Albano (central Italy). J Paleolimnol 26:283–292

Arnaud F, Révillon S, Debret M, Revel M, Chapron E, Jacob J, Giguet-Covex C, Poulenard J, Magny M (2012) Lake Bourget regional erosion patterns reconstruction reveals Holocene NW European Alps soil evolution and paleohydrology. Quat Sci Rev 51:81–92

Augustinus P, Cochran U, Kattel G, D'Costa D, Shane P (2012) Late Quaternary paleolimnology of Onepoto maar, Auckland, New Zealand: implications for the drivers of regional paleoclimate. Quat Int 253:18–31

Bacon C, Gardner J, Mayer L, Buktenica M, Dartnell P, Ramsey D, Robinson J (2002) Morphology, volcanism and mass wasting in Crater Lake, Oregon. Geol Soc Am Bull 114:675–692

Bani P, Join J-L, Cronin SJ, Lardy M, Rouet I, Garaebiti E (2009) Characteristics of the summit lakes of Ambae volcano and their potential for generating lahars. Nat Hazards Earth Syst Sci 9:1471–1478

Barbierro RP, Warren GJ (2011) Rotifer communities in the Laurentian Great Lakes, 1983–2006 and factors affecting their composition. J Great Lakes Res 37:528–540

Behar F, Beaumont V, Penteado HL, De B (2001) Rock-Eval 6 technology: performances and developments. Oil Gas Sci Technol – Rev IFP 56(2):111–134

Blaauw M (2010) Methods and code for 'classical' age-modelling of radiocarbon sequences. Quat Geochronol 5:512–518

Blomqvist P (2001) Phytoplankton responses to biomanipulated grazing pressure and nutrient additions – enclosure studies in unlimed and limed Lake Njupfatet, central Sweden. Environ Pollut 111:333–348

Bonhomme C, Poulin M, Vinçon-Leite B, Saad M, Groleau A, Jézéquel D, Tassin B (2011) Maintaining meromixis in Lake Pavin (Auvergne, France): the key role of sublacustrine spring. Compt Rendus Geosci 343:749–759

Brauer A, Endres C, Günter C, Litt T, Stebich M, Negendank JFW (1999) High resolution sediment and vegetation responses to Younger Dryas climate change in varved lake sediments from Meerfelder Maar, Germany. Quat Sci Rev 18(3):321–329

Caballero M, Vazquez G, Lozano-Garcia S, Rodriguez A, Sosa-Najera S, Ruiz-Fernandez AC, Ortega B (2006) Present limnological conditions and recents (ca. 340 yr) paleolimnology of a tropical lake in the Sierra de Los Tuxtlas, eastern Mexico. J Paleolimnol 35:83–97

Camus G, Michard G, Olive P, Boivin P, Desgranges P, Jezequel D, Meybeck M, Peyrus J-C, Vinson J-M, Viollier E, Kornprobst J (1993) Risques d'éruption gazeuse carbonique en Auvergne. Bull Soc Geol Fr 164(6):767–781

Caracausi A, Mario Nuccio P, Favara R, Nicolosi M, Paternoster M (2009) Gas hazard assessment at the Monticchio crater lakes of Mt. Vulture, a volcano in Southern Italy. Terra Nova 21:83–87

Chapron E, Beck C, Pourchet M, Deconinck JF (1999) 1822 earthquake-triggered homogenite in Lake Le Bourget (NW Alps). Terra Nova 11:86–92

Chapron E, Arnaud F, Noël H, Revel M, Desmet M, Perdereau L (2005) Rhône-river flood deposits in Lake Le Bourget: a proxy for Holocene environmental changes in the NW Alps, France. Boreas 34(4):404–416

Chapron E, Albéric P, Jézéquel D, Versteeg W, Bourdier J-L, Sitbon J (2010) Multidisciplinary characterization of sedimentary processes in a recent maar lake (Lake Pavin, French Massif Central) and implication for natural hazards. Nat Hazards Earth Syst Sci 10:1–13

Chapron E, Ledoux G, Simonneau A, Albéric P, St-Onge G, Lajeunesse P, Boivin P, Desmet M (2012) New evidence of Holocene Mass-Wasting events in recent volcanic lakes from the French Massif Central (Lakes Pavin, Montcineyre and Chauvet) and implications for natural hazards. In: Yamada Y (ed) Submarine mass movements and their consequences, vol 31, Advances in natural and technological hazards research. Springer, Dordrecht, pp 255–264

Chassiot L, Chapron E, Di Giovanni C, Lajeunesse P, Tachikawa K, Garcia M, Bard E (2016) Historical seismicity of the Mont Dore volcanic province (Auvergne, France) unraveled by a regional lacustrine investigation: new insights about lake sensitivity to earthquakes. Sediment Geol 339:134–150

Cugny C, Mazier F, Galop D (2010) Modern and fossil non-pollen palynomorphs from the Basque mountains (Western Pyrenees, France): the use of coprophilous fongi to reconstruct pastoral activity. Veg Hist Archaeobotany 19:391–408

Debret M, Desmet M, Balsam W, Copard Y, Francus P, Laj C (2006) Spectrophotometer analysis of Holocene sediments from an anoxic fjord: Saanich Inlet, British Columbia, Canada. Mar Geol 229:15–28

Debret M, Chapron E, Desmet M, Rolland-Revel M, Magand O, Trentesaux A, Bout-Roumazeille V, Nomade J, Arnaud F (2010) North western Alps Holocene paleohydrology recorded by flooding activity in Lake Le Bourget, France. Quat Sci Rev 29:2185–2200

Debret M, Sebag D, Desmet M, Balsam W, Copard Y, Mourier M, Susperrigui A-S, Arnaud F, Bentaleb I, Chapron E, Lallier-Vergès E, Winiarski T (2011) Spectrocolorimetric interpretation of sedimentary dynamics: the new "Q7/4 diagram". Earth Sci Rev 109:1–19

Delbecque A (1898) Les lacs français. Chamerot & Renouard, Paris, 436 p

Delibrias G, Guillier MT, Labeyrie J (1972) Gif natural radiocarbon measurements VII. Radiocarbon 14:280–320

Giresse P, Maley J, Kelts K (1991) Sedimentation and paleoenvironment in crater lake Barombi Mbo, Cameroon, during the last 25 000 years. Sediment Geol 71:151–175

Gutowski A, van de Weyer K, Hofmann G, Doege A (eds) (2011) Makrophyten und Phytobenthos Indikatoren für den ökologischen Gewässerzustand. Druckschrift des Sächsischen Landesamts für Umwelt, Landwirtschaft und Geologie des Freistaates Sachsen, Dresden, Mai 2012, 188 pp

Hindáková A (2009) On the occurrence of Achnanthes thermalis var. rumrichorum (Bacillariophyceae) in Slovakia. Fottea 9:193–198

Jézéquel D, Sarazin G, Prévot F, Viollier E, Groleau A, Michard G, Agrinier P, Albéric P, Binet S, Bergonzini L (2011) Bilan hydrique du lac Pavin. Revue des Sciences Naturelles d'Auvergne 74–75:67–90

Kulbe T, Niederreiter RJ (2003) Freeze coring of soft surface sediments at a water depth of several hundred meters. J Paleolimnol 29:257–263

Lambert J, Levret-Arbaret A, Czitrom G, Dubie J-Y, Godefroy P (1997) Les tremblements de terre en France. Editions BRGM, Orléans, 127 p

Lange-Bertalot H (2001) Navicula sensu stricto, 10 Genera separated from Navicula sensu lato Frustulia. Diatoms of Europe 2:526

Lavrieux M, Disnar J-R, Chapron E, Bréheret J-G, Jacob J, Miras Y, Reyss J-L, Andrieu-Ponel V, Arnaud F (2013) 6700 yr sedimentary record of climatic and anthropogenic signals in Lake Aydat (French Massif Central). The Holocene 23(9):1317–1328

Lotter AF, Bigler C (2000) Do diatoms in the Swiss Alps reflect the lenght of ice-cover? Aquat Sci 62:125–141

Magny M (2006) Holocene fluctuations of lake levels in west-central Europe: methods of reconstruction, regional patterns, palaeoclimatic significance and forcing factors. Encycl Quat Geol 3:1389–1399

Magny M, Haas JN (2004) A major widespread climatic change around 5300 cal. Yr BP ago at the time of the Alpine Iceman. J Quat Sci 19:423–430

Magny M, Combrieu Nebout N, de Beaulieu J-L, Bout-Roumazeilles V, Colombaroli D, Desprat S, Francke A, Joannin S, Peyron O, Revel M, Sadori L, Siani G, Sicre M, Samartin S, Simonneau A, Tinner W, Vannière B, Wagner B, Zanchetta G, Anselmetti F, Brugiapaglia E, Chapron E, Debret M, Desmet M, Didier J, Essallami L, Galop D, Gilli A, Haas JN, Kallel N, Millet L, Stock A, Turon J, Wirth S (2013) North-south paleohydrological contrasts in the central Mediterraenean during the Holocene: tentative synthesis and working hypotheses. Clim Past 9:1901–1967

Martin J-M (1985) The Pavin crater lake. In: Stumm Y (ed) Chemical processes in lakes. Wiley, New York, pp 169–188

Martin J-M, Meybeck M, Nijampurkar VN, Somayajulu BLK (1992) ^{210}Pb, ^{226}Ra and ^{32}Si in Pavin lake (Massif Central, France). Chem Geol 94:173–181

Martin-Puertas C, Brauer A, Dulski P, Brademann B (2012) Testing climate-proxy stationarity throughout the Holocene: an example from the varved sediments of Lake Meerfelder Maar (Germany). Quat Sci Rev 58:56–65

Miras Y, Laggoun-Defarge F, Guenet P, Richard H (2004) Multidisciplinary approach to changes in agro-pastoral activities since the Sub-boreal in the surroundings of the "narse d'Espinasse" (Puy-de-Dôme, French Massif Central). Veg Hist Archaeobot 13:91–103

Monecke K, Anselmetti F, Becker A, Sturm M, Giardini D (2004) The record of historic earthquakes in lakes sediments of Central Switzerland. Tectonophysics 394:21–40

Mott RW, Woods AW (2010) A model of overturn of CO2 laden lakes triggered by bottom mixing. J Volcanol Geotherm Res 192(3–4):151–158

Mulder T, Cochonat P (1996) Classification of offshore mass movements. J Sediment Res 66:43–57

Nomade J, Chapron E, Desmet M, Reyss JL, Arnaud F, Lignier V (2005) Reconstructing historical seismicity from lake sediments (Lake Laffrey, Western Alps, France). Terra Nova 17:350–357

Oldfield F (1996) The PASICLAS project: synthesis and overview. Memoire dell'instituto italiano di Idrobiologia 55:329–357

Reille M, Pons A, de Beaulieu J-L (1992) Late and postglacial vegetation, climate and human action in the French Massif Central. Laboratoire de Botanique Historique et Palynologie, Marseille

Reimer PJ, Bard E, Bayliss A, Warren Beck J, Blackwell PG, Bronk Ramsey C, Buck CE, Cheng H, Lawrence Edwards E, Friedrich M, Grootes PM, Guilderson TP, Haflidason H, Hajdas I, Hatté C, Heaton TJ, Hoffmann DL, Hogg AG, Hughen KA, Felix Kaiser K, Kromer B, Manning SW, Niu M, Reimer RW, Richards DA, Scott EM, Southon JR, Staff RA, Turney CSM, van der Plicht J (2013) IntCal13 and Marine13 radiocarbon age calibration curves 0–50,000 years cal BP Radiocarbon 55:1869-1887

Rioual P, Andrieu-Ponel V, de Beaulieu J-L, Reille M, Svobodovac H, Battarbee RW (2007) Diatom responses to limnological and climatic changes at Ribains Maar (French Massif Central) during the Eemian and Early Würm. Quat Sci Rev 26:1557–1609

Schettler G, Albéric P (2008) Laghi di Monticchio (Southern Italy, Region Basilicata): genesis of sediments - a geochemical study. J Paleolimnol 40:529–556

Schettler G, Schwab MJ, Stebich M (2007) A 700-year record of climate change based on geochemical and palynological data from varved sediments (Lac Pavin, France). Chem Geol 240:11–35

Schmid M, Halbwachs M, Wehrli B, Wüest A (2005) Weak mixing in Lake Kivu: new insights indicate increasing risk of uncontrolled gas eruption. Geochem Geophys Geosyst 6(7):1–11

Sifeddine A, Bertrand P, Lallier–Vergès E, Patience AJ (1996) Lacustrine organic fluxes and palaeoclimatic variations during the last 15 ka: lac du Bouchet (Massif Central, France). Quat Sci Rev 15:203–211

Sigurdsson H, Devine JD, Tchua FM, Presser FM, Pringle MKW, Evans WC (1987) Origin of lethal gas burst from Lake Monoun, Cameroun. J Volcanol Geotherm Res 31:1–16

Simonneau A, Chapron E, Vannière B, Wirth SB, Gilli A, Di Giovanni C, Anselmetti FS, Desmet M, Magny M (2013a) Mass-movement and flood-induced deposits in Lake Ledro, Southern Alps, Italy: implications for Holocene paleohydrology and natural hazards. Clim Past 9:825–840

Simonneau A, Chapron E, Courp T, Tachikawa K, Le Roux G, Baron S, Galop D, Garcia M, Di Giovanni C, Motellica-Heino M, Mazier F, Foucher A, Houet T, Desmet M, Bard E (2013b) Recent climatic and anthropogenic imprints on lacustrine systems in the Pyrenean Mountains inferred from minerogenic and organic clastic supply (Vicdessos valley, Pyrenees, France). The Holocene 23:1764–1777

Simonneau A, Chapron E, Garçon M, Winiarski T, Graz Y, Chauvel C, Debret M, Motelica-Heino M, Desmet M, Di Giovanni C (2014) Tracking Holocene glacial and high-altitude alpine environments fluctuations from minerogenic and organic markers in proglacial lake sediments (Lake Blanc Huez, Western Frenc Alps). Quat Sci Rev 89:27–43

Stebich M, Brüchmann C, Kulbe T, Negendank JFW (2005) Vegetation history, human impact and climate change during the last 700 years recorded in annually laminated sediments of Lac Pavin, France. Rev Palaeobot Palynol 133:115–133

Strasser M, Anselmetti F (2008) Mass-movement events stratigraphy in Lake Zurich: a record of varying seismic and environmental impacts. Beiträge zur Geologie der Schweiz, Geotechnische Serie 95:23–41

Tanasienko A, Yakutina O, Chumbaev A (2011) Effect of snow amount on runoff, soil los and suspended sediment during periods of snowmelt in Southern West Siberia. Catena 87:45–51

Thouveny N, de Beaulieu JL, Bonifay E, Creer KM, Guiot J, Icole M, Johnsen S, Jouzel J, Reille M, Williams T, Williamson D (1994) Climate variations in Europe over the past 140-Kyr deduced from rock magnetism. Nature 371:503–506

Truze E, Kelts K (1993) Sedimentology and Paleoenvironment from the maar lac du Bouchet for the last climatic cycle, 0–120,000 years (Massif Central, France). In: Negendank JFW, Zolitschka B (eds) Paleolimnology of European Maar Lakes, vol 49, Lecture notes in earth sciences., pp 237–375

Van Dam H, Mertens A, Sinkeldam J (1994) A coded checklist and ecological indicator values of freshwater diatoms from the Netherlands. Neth J Aquat Ecol 28:117–133

Viollier E, Albéric P, Jezequel D, Michard G, Pèpe M, Sarazin G (1995) Geochemical study of a crater lake: the Pavin Lake, France-trace element behavior in the monimolimnion. Chem Geol 125:1–72

Voigt R, Grüger E, Baier J, Meischner D (2008) Seasonal variability of Holocene climate: a palaeolimnological study on varved sediments in Lake Jues (Harz Mountains, Germany). J Paleolimnol 40:1021–1052

Walker IR, Paterson CG (1986) Associations of diatoms in the surficial sediments of lakes and peat pools in Atlantic Canada. Hydrobiologia 134:265–272

Zolitschka B, Anselmetti F, Ariztegui D, Corbella H, Francus P, Lücke A, Maidana NI, Ohlendorf C, Schäbitz F, Wastegard S (2013) Environment and climate of the last 51000 years – New insights from the Potrok Aike maar lake Sediment Archive Drilling prOject (PASADO). Quat Sci Rev 71:1–12